

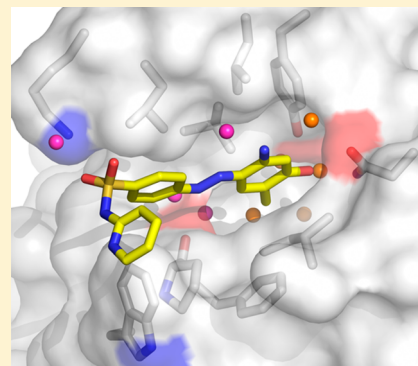
Structure-Guided Design of Potent Diazobenzene Inhibitors for the BET Bromodomains

Guangtao Zhang, Alexander N. Plotnikov, Elena Rusinova, Tong Shen, Keita Morohashi, Jennifer Joshua, Lei Zeng, Shiraz Mujtaba, Michael Ohlmeyer, and Ming-Ming Zhou*

Department of Structural and Chemical Biology, Icahn School of Medicine at Mount Sinai, 1425 Madison Avenue, New York, New York 10029, United States

S Supporting Information

ABSTRACT: BRD4, characterized by two acetyl-lysine binding bromodomains and an extra-terminal (ET) domain, is a key chromatin organizer that directs gene activation in chromatin through transcription factor recruitment, enhancer assembly, and pause release of the RNA polymerase II complex for transcription elongation. BRD4 has been recently validated as a new epigenetic drug target for cancer and inflammation. Our current knowledge of the functional differences of the two bromodomains of BRD4, however, is limited and is hindered by the lack of selective inhibitors. Here, we report our structure-guided development of diazobenzene-based small-molecule inhibitors for the BRD4 bromodomains that have over 90% sequence identity at the acetyl-lysine binding site. Our lead compound, MS436, through a set of water-mediated interactions, exhibits low nanomolar affinity (estimated K_i of 30–50 nM), with preference for the first bromodomain over the second. We demonstrated that MS436 effectively inhibits BRD4 activity in NF- κ B-directed production of nitric oxide and proinflammatory cytokine interleukin-6 in murine macrophages. MS436 represents a new class of bromodomain inhibitors and will facilitate further investigation of the biological functions of the two bromodomains of BRD4 in gene expression.



■ INTRODUCTION

Human DNA is tightly packaged into chromatin by wrapping around the core histone octamer of nucleosomes. The N- and C-termini of the core histones, protruding out from the nucleosome, are subject to a wide variety of post-translational amino acid modifications including acetylation, methylation, phosphorylation, ubiquitinylation, and SUMOylation.¹ These chemical modifications of the histones, in combination with DNA modifications, function in a synergistic fashion to regulate gene activation or silencing in chromatin. The ϵ -N-acetylation of lysine neutralizes positive charges on histones, weakening their interactions with negatively charged DNA. Site-specific lysine acetylation also plays an active role in transitioning chromatin into a relaxed state and directing the recruitment of the gene transcriptional machinery complex for gene activation.

The evolutionarily conserved bromodomain (BrD) serves as the acetyl-lysine binding domain^{2,3} to regulate gene activation in chromatin. The 61 human bromodomains embedded in 46 proteins⁴ are divided into eight subfamilies with distinctive features based on sequence similarities.⁵ One major group is BET (bromodomain and extra-terminal domain) proteins composed of BRD2, BRD3, BRD4, and BRDT, each of which contains two tandem bromodomains (BrD1 and BrD2). All bromodomains share a conserved left-handed helix-bundle that is made out of four α helices, named α Z, α A, α B, and α C, respectively. The interhelical loop regions, known as the ZA and BC loops, form the acetyl-lysine binding pocket that is

located at one end of the helix bundle. The amino acid residues in the acetyl-lysine binding pocket are highly conserved, with over 90% sequence identity between the two bromodomains in each BET proteins. Of these is a highly conserved Asn residue that is essential for lysine-acetylated histone recognition by forming a hydrogen bond to the acetyl amide group of the acetylated lysine.

BRD4, arguably the most extensively characterized BET protein, has been implicated in functions in a wide array of human disorders including cancer,^{6–8} obesity,⁹ kidney disease,¹⁰ lung fibrosis,¹¹ and other inflammatory diseases.¹² There is growing evidence that the two bromodomains of BRD4 have different biological functions.^{10,12,13} Despite several potent BET inhibitors reported in recent studies,^{6,7,10,14–17} there is still no small-molecule inhibitor shown to be capable of differentiating between the two bromodomains within any individual BET protein. Developing such a selective inhibitor is a challenging task because of the extremely high sequence identity of these bromodomains, particularly at their acetyl-lysine binding pockets.

In this study, we report the structure-guided development of a new class of potent and selective diazobenzene-based small-molecule inhibitors for the BET bromodomains. Our ligand design started with a diazobenzene compound MS120,

Received: September 2, 2013

Published: October 21, 2013

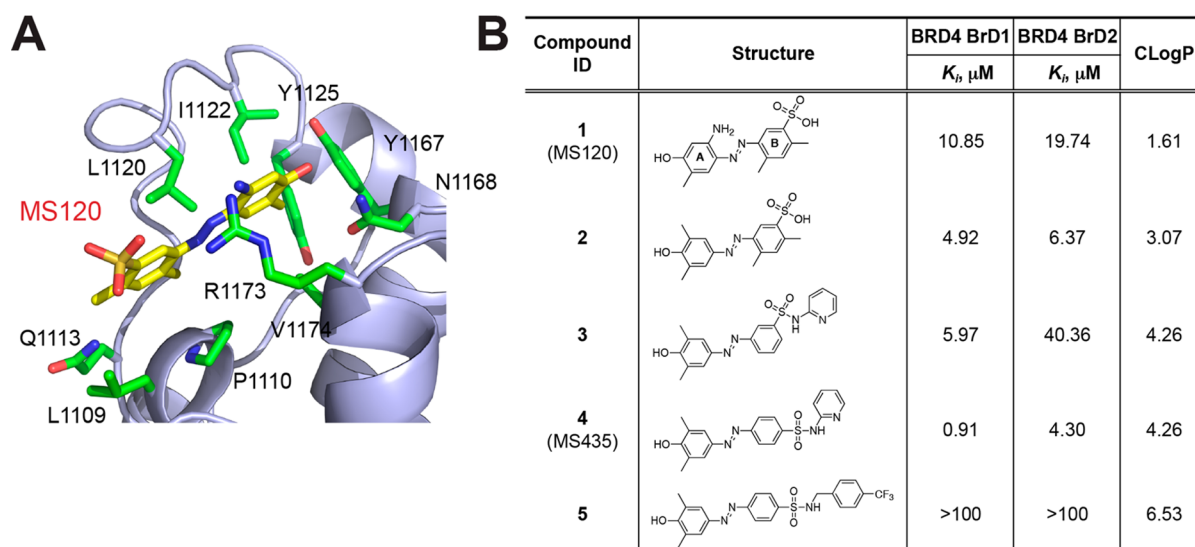


Figure 1. Structure-guided development of diazobenzene-based BrD inhibitors. (A) Three-dimensional solution structure of the BrD inhibitor MS120 (yellow) bound to the CBP BrD (PDB: 2L84). The key amino acid residues in the acetyl-lysine binding site are shown in sticks. (B) Structure–activity relationship table illustrating binding affinity of a select number of diazobenzene-based BrD inhibitors to the two BrDs of BRD4. CLogP values were calculated using ChemBioDraw Ultra 12.0.

Table 1. Structure–Activity Relationship of C Ring Analogues of Diazobenzenes

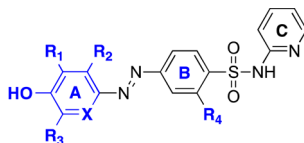
Compound ID	R_5	R_6	R_7	R_8	Y	BRD4 BrD1	BRD4 BrD2	CLogP ^a
						K_b , μM	K_b , μM	
6	Me	H	H	H	N	7.89	7.12	4.91
7	H	H	H	CF ₃	C	6.13	7.77	6.54
8	H	Cl	H	H	N	0.90	5.92	5.40
9	H	H	COOH	H	N	0.32	1.38	4.37
10	H	H	Cl	H	N	0.73	5.84	5.40
11	H	H	Br	H	N	6.54	38.7	5.67
12	H	H	OMe	H	N	0.50	2.23	4.66
13	H	H	OMe	H	C	6.48	6.59	5.50
14	H	H	CF ₃	H	C	10.7	7.14	6.54
15	H	H		H	C	9.60	12.2	4.37
16	H	H	F	H	N	1.30	3.44	4.45
17	H	H	F	H	C	1.84	8.87	5.75

^aCLogP values were calculated using ChemBioDraw Ultra 12.0.

originally discovered as an inhibitor for the CBP BrD.¹⁸ Guided by our new structural insights into recognition of the

diazobenzenes by both CBP and BRD4 BrDs, we designed specific chemical modifications to acquire lead selectivity

Table 2. Structure–Activity Relationship of the A or B Ring Analogues of Diazobenzenes



Compound ID	R ₁	R ₂	R ₃	R ₄	X	BRD4 BrD1	BRD4 BrD2	CLogP
						K _i , μM	K _p , μM	
18	Me	H	Me	OMe	C	3.13	7.77	3.82
19	Cl	H	Cl	H	C	1.27	4.89	4.27
20	Br	H	Me	H	C	2.79	4.48	4.50
21	Cl	H	Me	H	C	1.40	4.81	4.30
22	Br	H	H	H	C	4.67	4.69	4.05
23	Cl	H	H	H	C	1.30	6.16	3.85
24	Me	H	H	H	C	6.43	8.20	3.81
25	Br	H	Br	H	C	0.52	4.29	4.67
26	CF ₃	H	H	H	C	9.45	6.83	4.35
27 (MS436)	H	NH ₂	Me	H	C	<0.085	0.34	2.65
28 (MS267)	Me	NH ₂	Me	H	C	0.15	0.44	3.05
29 (MS363)	Cl	NH ₂	Me	H	C	0.17	0.64	3.17
30	H	NH ₂	OMe	H	C	1.28	5.39	1.96
31	Me	H	Me	H	N	2.31	24.60	4.44
32	Me	Me	Me	H	N	6.02	9.10	4.92
33	Me	H	OH	H	C	2.39	3.27	3.29
34	H	H	OH	H	C	4.59	3.91	2.84

toward BRD4 BrDs and conducted extensive structure–activity relationship studies. Our lead compound MS436 exhibits potent affinity of an estimated K_i of 30–50 nM for BRD4 BrD1 and a 10-fold selectivity over the BrD2, which is achieved through a unique set of water-mediated intermolecular interactions. We further demonstrated cellular efficacy of our lead diazobenzene inhibitors in blocking BRD4 transcriptional activity in NF-κB-directed production of nitric oxide and proinflammatory cytokine interleukin-6 in murine macrophages. We expect that this new class of bromodomain inhibitors will facilitate further mechanistic investigation of the biological functions of the two bromodomains of BRD4 in gene activation in human biology and disease.

RESULTS AND DISCUSSION

Structure-Guided Design of Diazobenzenes as BET Bromodomain Inhibitors. We have previously reported MS120 (compound 1, Figure 1), (*E*)-5-((2-amino-4-hydroxy-

5-methylphenyl)diazonyl)-2,4-dimethylbenzenesulfonic acid, as a small-molecule inhibitor for the bromodomain of HAT coactivator CBP.¹⁸ This compound shows modest activity as assessed in a fluorescent polarization assay toward BRD4 BrD1. The NMR solution structure of the CBP BrD/MS120 complex (PDB: 2L84) reveals that MS120 binds at the acetyl-lysine binding pocket with the phenolic hydroxyl group, forming a hydrogen bond with the amide nitrogen on the side chain of Asn1168 of the BrD. This Asn residue is critically important in acetyl-lysine binding and is highly conserved in the bromodomain family.³ The overall molecule fits in the narrow groove constituted by the interhelical ZA and BC loops in which both the sulfonate and the amino groups are locked by a pair of electrostatic interactions with the guanidinium group of Arg1173 in the BC loop, a unique residue in the CBP BrD (Figure 1A). Our structure-based sequence analysis suggested chemical modifications to engineer this diazobenzene scaffold compound to be selective inhibitors for the BET bromodo-

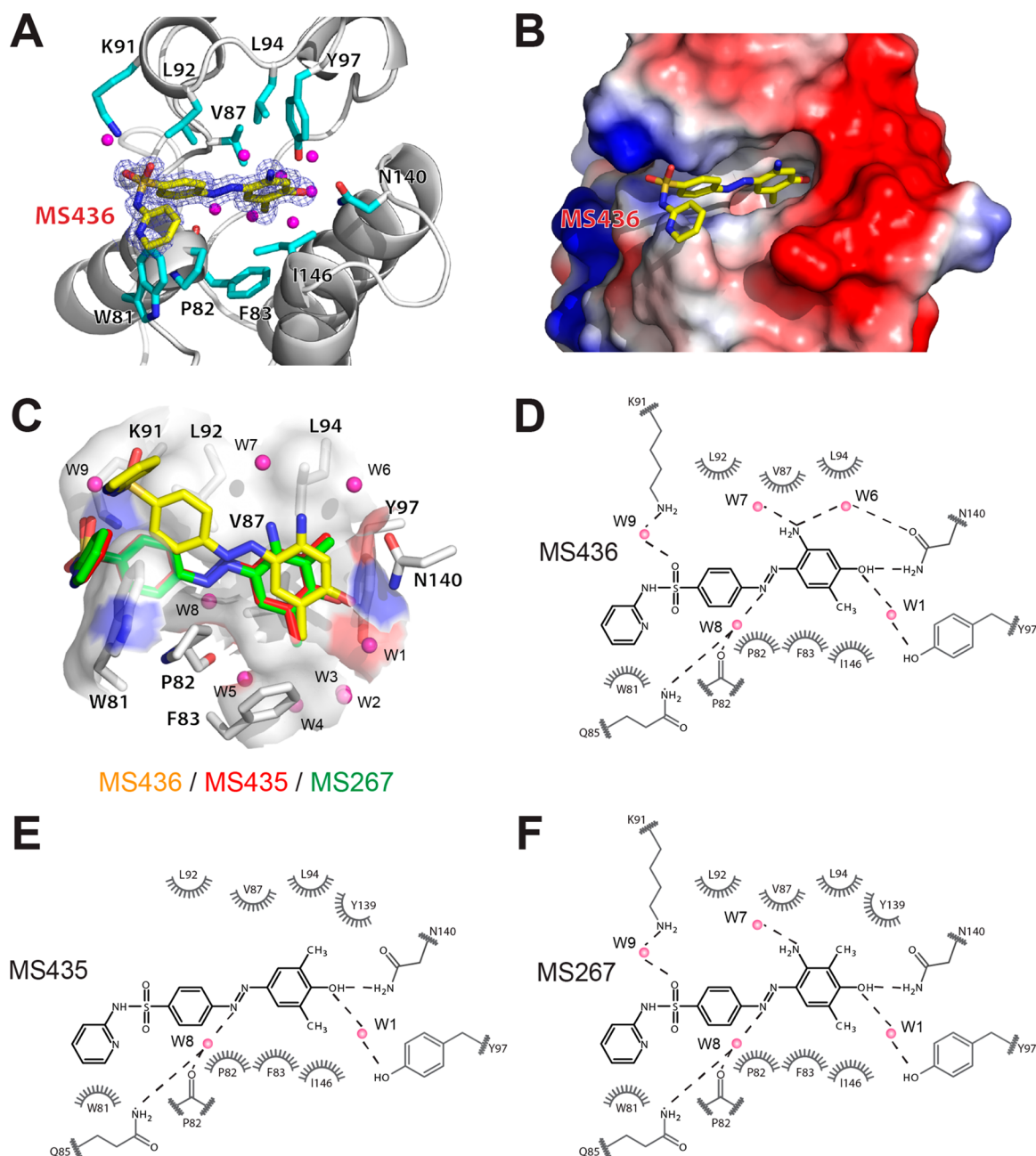


Figure 2. Molecular basis of the BRD4 BrD1 recognition of the lead diazobenzene-based BrD inhibitors. (A) Three-dimensional crystal structure of MS436 (yellow) bound to BRD4-BrD1, depicted in a ribbon diagram. Key amino acid residues at the acetyl-lysine binding site are shown in sticks. Ligand MS436 is color-coded by atom type. (B) Electrostatic surface representation of BRD4-BrD1 bound to MS436. (C) Superimposition of MS436, MS435, and MS267 when bound to BRD4-BrD1. Only the MS436-bound protein structure is shown. Side chains of the key residues involved in ligand binding are depicted in sticks and color-coded by atom type. The bound water molecules are shown as spheres in magenta. (D–F) Schematic diagrams highlighting key interactions in the BRD4 BrD1 recognition of MS436, MS435, and MS267, respectively. Water molecules are shown in magenta spheres, and hydrogen bonds are drawn in dashed line. The figure was generated using the program LIGPLOT.³²

mains. For example, additional π - π interactions may be established between the ligand and Trp81 in the BRD4 BrD1, which corresponds to Leu1109 of CBP. The acetyl-lysine binding pocket of the BRD4 BrD1 is larger in volume than that of the CBP BrD, thus allowing further modifications to build target selectivity.⁵

Chemical Synthesis of Diazobenzene-Based Bromodomain Inhibitors. On the basis of the structure-guided design, we first extended the diazobenzene by adding a ring to benzenesulfonate (Figure 1B). In this case, we constructed the extended molecule based on 2, a MS120 analogue, which itself

showed a 2- to 3-fold improvement in binding affinity to the BRD4 BrDs over MS120 (1). The synthetic schemes and procedures are described in detail in the Materials and Methods. The binding affinity of these newly synthesized compounds for various bromodomain proteins was assessed using a fluorescence anisotropy binding assay as described previously.¹⁰ Specifically, 3, an analogue of 2, inherited the sulfonyl group at the meta position and extended the system by coupling to 2-aminopyridine. 3 retained the affinity of 2, indicating extension at the meta position is tolerated. Interestingly, as the sulfonamide was repositioned to the para

position, the affinity for the BRD4 BrD1 was improved by over 6-fold (MS435, 4 vs 3). However, when we attempted trifluoromethyl-benzylamine as an alternative ring system with an extra carbon in the linker (5 in Figure 1B and 35 and 36 in Supporting Information Table 1), the inhibitory capacity deteriorated drastically. Therefore, we adopted the optimized 2-aminopyridine as a model system as we continued our lead-optimization campaign.

Structure–Activity Relationship of the C Ring.

Encouraged by the initial results, we commenced an investigation of the structure–activity relationship (SAR) on the C ring toward BRD4 BrD1 (Table 1). Hydrogen on R₅ is required; substitution of H with a methyl group resulted in a 9-fold loss in activity (6 vs MS435). Substitution at this position possibly causes a steric collision with Pro82 (see below). Although substitutions at R₆ and R₈ are generally not tolerated (7 and 8 vs MS435), substitutions at R₇ are well tolerated. In particular, electron-withdrawing groups at R₇, such as the carboxyl group in compound 9, displayed activities with about a 3-fold higher affinity than MS435. Chlorine substitution at R₇ (10) was tolerated; however, when bromine was introduced instead (11), the inhibitory activity toward BRD4 BrD1 declined by 10-fold. The nitrogen on the C ring is preferred, and corresponding carbon analogues displayed lower affinity (for example, 11 or 12 vs 13, 14, or 15; 16 vs 17). Notably, we observed that the nitrogen in the C ring resulted in a 13-fold improvement in binding affinity to BRD4 BrD1, whereas there was a 3-fold increase for BRD4 BrD2, thus yielding an overall 4-fold binding selectivity between these two BrDs (12 vs 13). Nonsubstituted 2-aminopyridine was one of the best pieces in the C ring. Considering its simplicity, stability, and potential impact on the selectivity between the BrD1 and BrD2 of BRD4, we decided to choose 2-aminopyridine as a conserved moiety as we continued to optimize the A and B rings.

Structure–Activity Relationship of the A and B Rings.

Substitutions on the B ring, such as a methoxyl group, did not lead to tighter binding (18 vs MS435) (Table 2). Analysis of the crystal structure of MS435 bound to BRD4 BrD1 (Figure 2C) revealed that the hydroxyl group on the phenol ring was hydrogen bonded to the conserved Asn140. Hence, we primarily concentrated on the optimization of the A ring and built a focused library of over 30 diazobenzene compounds.

We first examined the importance of the hydroxyl group on the A ring. When it was replaced with a methoxy (37) or an acetamide group (38) (Supporting Information Table 1), the resulting compounds completely lost binding activity, confirming our structural analysis. Detailed study further revealed that bulky groups such as *t*-butyl and isopropyl at R₁ and R₃ are not tolerated. When one bulky group was introduced (39 and 40 in Supporting Information Table 1), the affinity decreased about 10-fold as compared to MS435; when two bulky groups were introduced simultaneously (41 and 42), the compounds almost completely lost their activities (Supporting Information Table 1). The limited space in the acetyl-lysine binding pocket simply cannot accommodate large functional groups. For the same reason, bicyclic (43–46) systems did not show good activities toward BRD4 BrD1. Flexible substitutions such as amino-methyl and hydroxymethyl were also not tolerated (47–49 in Supporting Information Table 1). However, halides, especially bromides, are generally tolerated, such as in compounds 19–25 (Table 2). It is worth pointing out that symmetrically bisubstituted phenols appear to outperform their monosubstituted counterparts, suggesting that steric hindrance con-

strains the rotational freedom between the A ring and diazo linker, locking the substituted A ring in a more favorable conformation. Strong electron-withdrawing groups, such as CF₃ (26, Table 2), likely weakens the hydrogen bond between phenolic OH and Asn140 and is therefore not preferred.

Notably, MS436 (27) is the most potent compound of this set of diazobenzene compounds, as determined in an *in vitro* fluorescent anisotropy assay, with a K_i value of better than 85 nM for BRD4 BrD1 (limited by the binding affinity of the assay probe; the estimated K_i is 30–50 nM) and an approximately 10-fold selectivity for BrD1 over BrD2 of BRD4 (Table 2). This is the first reported low-nanomolar affinity BrD inhibitor with clear selectivity between these two BrDs of BRD4 as far as we know. MS436 is 10 times more potent than model compound MS435 toward BRD4 BrD1. Interestingly, MS267 (28), a hybrid compound incorporating the key features of MS435 and MS436, exhibited about a 2-fold reduction in potency compared to MS436, although it is still much better than MS435. In addition, placing a Cl at the ortho position with respect to the hydroxyl group in the A ring in another hybrid compound, MS363 (29), showed a 2-fold decrease in binding affinity for both BrDs of BRD4. Nevertheless, both MS267 and MS363 maintained the selectivity for BRD4 BrD1 over BrD2. Notably, a change of the methyl group at R₃ in MS436 to methoxy (30) resulted in a 15-fold decrease in the binding affinity to either BRD4 BrD1 or BrD2. This explains the importance of this methyl group in mimicking the methyl group of acetyl-lysine in a biological ligand. Finally, our endeavors to employ heterocycles in the A ring were unfruitful. Introduction of a nitrogen atom into the A ring aromatic system led to a 3-fold decrease in the affinity (31 and 32 vs MS435).

Structural Basis for Ligand Selectivity. We solved three high-resolution crystal structures of BRD4 BrD1 bound to MS436, MS435, or MS267 to determine the molecular basis of the binding affinity and selectivity of these lead BrD inhibitors (Figure 2A–F). In a similar orientation to that of MS120 in the CBP BrD, these much improved diazobenzene inhibitors bind across the acetyl-lysine binding pocket in the ZA and BC loops in BRD4 BrD1. The hydroxyl group in the A ring forms a hydrogen bond to the amide of the conserved Asn140 and another water (W1)-mediated hydrogen bond to the phenoxy group for Tyr97 (Figure 2C–F). In addition, the second nitrogen in the diazo linker is engaged in a water (W8)-mediated hydrogen bond to the backbone carbonyl oxygen of the conserved Pro82 that plays an important structural role in many BrDs.³ The core diazobenzene moiety is sandwiched between hydrophobic walls formed by Val87, Leu92, Leu94, and Tyr139 on one side and Pro82, Phe83 and Ile146 on the other. Furthermore, the pyridine ring (C ring), particularly in MS435 and MS267, forms π – π interactions with the side-chain *idol* of Trp81. Collectively, these intermolecular interactions explain the diazobenzene scaffold as a preferred platform as BrD inhibitors for BRD4.

Notably, besides five water molecules (W1–W5) commonly observed in BrDs and stably located at the bottom of the acetyl-lysine binding pocket,³ we observed several more bound water molecules that are intimately engaged in ligand recognition with these diazobenzene inhibitors, particularly for MS436 (Figure 2C). Specifically, in addition to W8, which facilitates a water-mediated hydrogen bond between one nitrogen atom of the diazo linker and carbonyl oxygen of Pro82 as described above for all three BrD inhibitors, MS436-bound structure

reveals three additional water molecules. For example, W6 bridges hydrogen-bonding interactions between the amino group of the A ring and carbonyl oxygen of the conserved Asn140; the former is engaged in a hydrogen bond with another surface-exposed bound water, W7. In addition, W9 establishes a set of hydrogen-bonding interactions between the sulfonamide oxygen in the B–C ring linker and the side-chain amine of Lys91. The latter is one of very few unique residues in the BrD1 of BRD4; the corresponding residue in the BrD2 is Ala384. Notably, when the 2-aminopyridine sulfonamide (C ring) connectivity to the B ring was moved to meta position to the diazo linker, we observed a 10- or 3-fold reduction in binding affinity to BRD4 BrD1 and BrD2, respectively (S1 vs MS436, see Supporting Information Table 1). Finally, W6, W7, and W9 are missing in the MS435-bound structure, whereas only W7 and W9 are present in the MS267 structure.

The protein structures of BRD4 BrD1 bound to these diazobenzene inhibitors are nearly identical. Superimposition of these structures reveals that MS435 and MS267 are bound in an almost identical position and orientation, whereas MS436 is upward shifted, anchoring on the hydroxyl group of the A ring, which is positioned at nearly same position in the protein with all three ligands (Figure 2C). This shift of MS436 resulted in an increased distance between the pyridine ring (C ring) and Trp81 as compared to that in MS435 or MS267 but yielded additional hydrogen-bonding interactions involving W6, W7, and W9 as compared to MS435 (Figure 2D vs 2E,F). In addition, W8 and W9 in the MS436-bound structure are repositioned accordingly to maintain hydrogen bonds between the protein residues and the ligand as described above. Most notably, the key hydrogen bond formed between the hydroxyl group in the A ring and the amide of Asn140 is reduced to 2.8 Å in MS436 from 3.0 Å in MS435 and MS267. Taken together, these structural insights explain the detailed molecular basis for the potent binding affinity of MS436 that is superior to MS435 and MS267 as a selective BrD inhibitor for BrD1 over BrD2 of BRD4.

Activity of Diazobenzene Compounds against the Bromodomain Panel. We profiled four lead diazobenzene-based BET BrD inhibitors, MS435, MS436, MS267, and MS363, against a panel of bromodomains that represent different subgroups of the human bromodomain family (Table 3). All four inhibitors preferentially bind to the BrDs of BRD4 and BRD3 over the other BrDs tested. Notably, MS436 activity toward CBP BrD is four times better than initial compound MS120. It is worth mentioning that these diazobenzene

Table 3. Lead BrD Inhibitors against a Panel of BrDs

BrD protein	27 (MS436) K_i , μM	4 (MS435) K_i , μM	28 (MS267) K_i , μM	29 (MS363) K_i , μM
BRD4-BrD1 ^a	<0.085	0.91	0.15	0.17
BRD4-BrD2 ^a	0.34	4.30	0.45	0.64
BRD3-BrD1 ^a	0.10	1.64	0.29	0.24
BRD3-BrD2 ^a	0.14	2.48	0.22	0.32
CBP BrD ^b	2.18	7.15	5.12	5.59
PCAF ^c	5.52		<3.34	<3.34
BRD7 ^b	2.72	3.54	<1.43	<1.43
BPTF ^c	6.06		<1.7	1.62
BAZ2b ^c	3.29		2.26	3.30
SMARCA4 ^c	7.97	<6.56	<6.56	<6.56

Note: Assay probe used: ^aMS574; ^bMS226; ^cMS239 (see details in Materials and Methods).

compounds have a different bromodomain activity profile from diazepine-based BrD inhibitors such as JQ1,⁶ MS417,¹⁰ and I-BET.⁷ Specifically, MS267 showed binding affinity K_i values of <1.43, <1.70, and 2.26 μM for the BrDs of BRD7, BPTF, and BAZ2b, respectively. MS435 showed a K_i value of <6.56 μM for SMARCA4 BrD. These unique activity profiles make them potentially useful probes for studies of these non-BET BrDs.

Physicochemical Properties of the Top Diazobenzene Bromodomain Inhibitors. We evaluated the physicochemical properties, including CLogP and lipophilic ligand efficiency (LLE),¹⁹ of our top four diazobenzene-based bromodomain inhibitors, MS435, MS436, MS267, and MS363, to understand further their potential in cellular study. Of these, MS436 shows the best physicochemical properties (Table 4). As suggested in

Table 4. Physicochemical Properties of Compounds against BRD4-BrD1

ID	compound	K_i , μM	p <i>K_i</i>	CLogP	lipophilic ligand efficiency
27	MS436	<0.0845	7.07	2.65	>4.42
4	MS435	0.91	6.04	4.26	1.78
28	MS267	0.15	6.82	3.05	3.77
29	MS363	0.17	6.77	3.17	3.60

recent toxicology studies, compounds with CLogP <3 have much lower potential adverse effects in vivo.^{20,21} MS436 has CLogP of 2.65, thus belonging to the low-risk category. MS436 strikes a good balance between lipophilicity and potency. The lipophilic ligand efficiency of MS436 (LLE = 4.42) is also well above the other diazobenzene analogues and is in line with the most probable LLE distribution (2–6) as reported in a recent statistical analysis of successful drug molecules.¹⁹

Activities of Diazobenzene Compounds in Murine Macrophage RAW264.7 Cells. These four lead diazobenzene bromodomain inhibitors exhibited little observable cytotoxicity on cell growth and proliferation, as determined in an MTT assay in murine macrophage RAW264.7 cells. As shown by this MTT study, the cell viability was fairly stable with these bromodomain inhibitors at concentrations up to 100 μM (Figure 3A). We next evaluated the cellular efficacy of these bromodomain inhibitors in blocking BRD4 functions in gene transcription. Nitric oxide synthase (NOS) catalyzes a stoichiometric production of nitric oxide (NO) from L-arginine in cells. NO production in macrophages is mediated by inducible nitric oxide synthase (iNOS), which is regulated by the NF- κB pathway.²² As shown in our recent study, NF- κB transcriptional activity for target-gene activation is dependent upon its lysine-acetylation-mediated interactions with BRD4,¹⁰ which recruits the activated NF- κB to its target gene sites by binding to diacetylated histone H4, particularly H4K5ac/K8ac. Indeed, we observed that treatment with the diazobenzene compounds in a dose-dependent manner blocked NF- κB -directed NO production in RAW264.7 cells upon LPS stimulation (Figure 3B). In agreement with their in vitro binding affinity to the BRD4 BrD1, MS436 showed a more profound inhibitory activity on NO production than MS435. Consistent with the fact that the BET proteins are functionally vital for macrophage inflammatory responses,²³ these diazobenzene bromodomain inhibitors effectively block LPS-induced proinflammatory cytokine interleukin (IL)-6 expression in the macrophage cells, as illustrated in an ELISA assay (Figure 3C), of which MS436 and MS363 showed the most profound

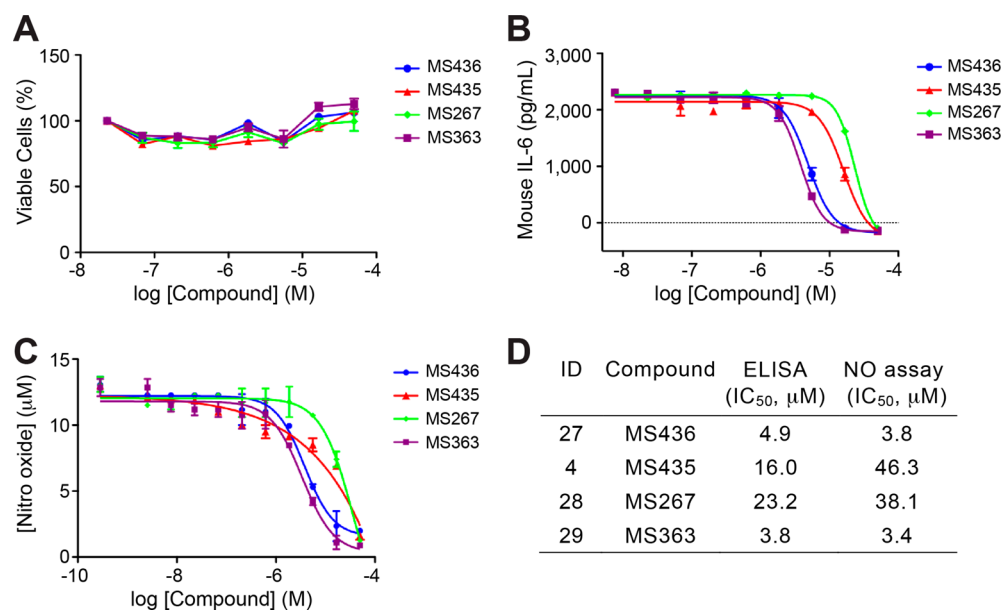


Figure 3. Characterization of effects of the diazobenzene BrD inhibitors on BRD4 function in gene transcription. (A) Effects of cell viability on the BrD inhibitors in murine macrophage RAW264.7 cells. Mitochondrial respiration, an indicator of cell viability, was assayed by the mitochondrial-dependent reduction of MTT to formazan. (B) Effects of the BrD inhibitors on LPS-induced IL-6 secretion in murine macrophage RAW264.7 cells. (C) Effects of the BrD inhibitors on LPS-induced NO production in murine macrophage RAW264.7 cells. (D) Estimated efficiency of the four lead BrD inhibitors in the cellular assays as described in panels B and C.

inhibitory activity, which was similar to their activity in the NO inhibition study. Taken together, these results demonstrate that these lead diazobenzene bromodomain inhibitors, particularly MS436, can effectively modulate BRD4 functions in gene transcriptional activation in cells.

CONCLUSIONS

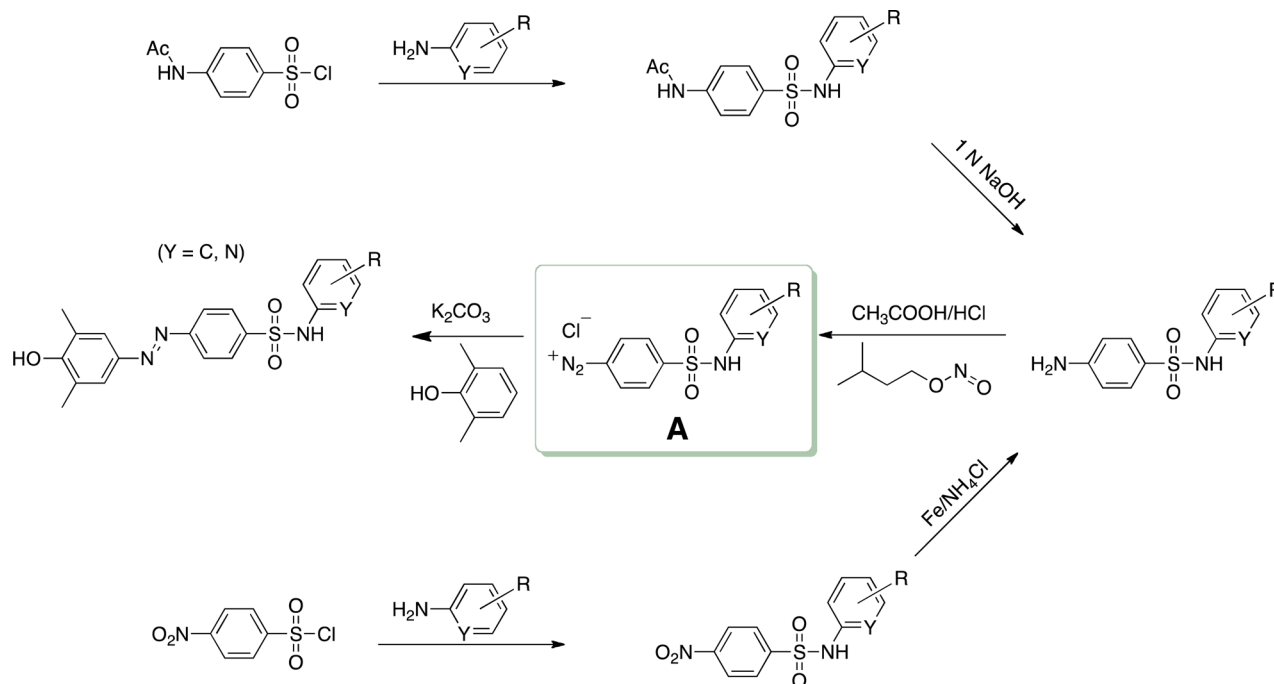
In this study, we report our structure-guided development of a new class of diazobenzene-based small-molecule inhibitors for the BET bromodomains. MS436 is the best inhibitor yielded from our extensive lead optimization using a combined medicinal chemistry and structure–activity relationship study. We improved the affinity of the diazobenzene compounds toward BRD4 BrD1 by over 100-fold. MS436 has an estimated K_i of 30–50 nM for BRD4 BrD1, with a 10-fold selectivity over BrD2. These lead diazobenzene compounds possess preferable druglike properties. We further demonstrated the cellular efficacy of four lead diazobenzene BrD inhibitors in inhibiting BRD4 transcriptional activity in LPS-activated, NF- κ B-directed production of nitric oxide and proinflammatory cytokine IL-6 in murine macrophage RAW264.7 cells. To our knowledge, MS436 is the first low-nanomolar small-molecule bromodomain inhibitor that is selective between the two structurally highly similar BrDs of BRD4. It compares favorably to the other recently reported BRD4 BrD inhibitors such as 3,4-dihydro-3-methyl-2(1*H*)-quinazolinones²⁴ and 3,5-dimethoxyisoxazole,¹⁴ which do not show selectivity between the two BrDs of BRD4.

Our detailed high-resolution crystal structural analysis of the BRD4 BrD1 bound to the lead diazobenzene ligands reveals that the residues in the acetyl-lysine binding pocket adopt a rather rigid conformation that is not influenced significantly upon binding to different small-molecule ligands or the acetylated-lysine in a histone peptide (Figure 2). Surprisingly, we found that a set of structurally bound water molecules work together to direct ligand recognition through bridging multiple

water-mediated hydrogen-bonding interactions between the key conserved residues and a bound ligand. It is interesting to note that through such versatile and cooperative activity, bound water molecules play a direct role in ligand recognition by the bromodomains. These observations likely reflect the dynamic and transient nature of acetyl-lysine binding by the bromodomains, which is necessary for directing the protein–protein interactions required for gene transcriptional activation on-demand and in an ordered fashion in the context of chromatin.

Unlike other bromodomains of the HAT coactivators PCAF and CBP/p300, the BET bromodomains distinctly prefer to interact with multilycine acetylation sites in histones and transcription-associated proteins. Growing evidence from our studies and others suggest that the two bromodomains of BRD4 are engaged in different molecular functions for the control of gene transcriptional activation in chromatin.^{10,12,13} Specifically, the first bromodomain of BRD4 binds to hyperacetylated histone H4 by recognizing H4K5ac/K8ac, a dual-acetylation mark that signals for gene activation, whereas the second bromodomain functions to recruit activated and lysine-acetylated transcription factors to target gene promoter and enhancer sites as well as to bridge triacetylated cyclin T1 of p-TEFb to RNA polymerase II to establish an activated transcriptional-machinery complex for productive transcriptional elongation. Our new diazobenzene-based bromodomain inhibitors that are potent and selective for these two BrDs of BRD4, particularly MS436, and should facilitate further mechanistic investigation of specific functions of the two bromodomains of BRD4 in various physiological and pathophysiological contexts. Such studies are needed to guide the future development of novel and safe small-molecule BRD4 inhibitors as new targeted epigenetic therapies to treat human disorders including cancer and inflammation.

Scheme 1. General Synthetic Scheme for C Ring Analogues of Diazobenzene



MATERIALS AND METHODS

Protein Preparation. Expression and purification of the recombinant bromodomains of various transcriptional proteins in poly-His tagged form were performed using a procedure described previously.¹⁰ The protein was purified by affinity chromatography on a nickel-IDA column (Invitrogen) followed by the removal of the poly-His tag by thrombin cleavage.

Fluorescence Anisotropy Binding Assay. Binding affinity of the newly synthesized diazobenzene compounds for various bromodomains was assessed in a fluorescence anisotropy competition assay using fluorescein-labeled MS417 (MS574) as an assay probe for BET BrDs, as described previously.¹⁰ For non-BET BrDs, different fluorescein-labeled probes (unpublished data, M.-M.Z.), were used as indicated in Table 3. Competition experiments were performed with a BrD protein (0.25–1 μ M) and the fluorescent probe (80 nM) and increasing concentration of unlabeled competing ligand in a PBS buffer (pH 7.4) in total volume of 80 μ L. Measurements were obtained after a 1 h incubation of the fluorescent ligand and the protein at 25 $^{\circ}$ C with a Safire 2 microplate reader (Tecan, Research Triangle Park, NC). In a competition-binding assay, the fluorescent ligand concentration was $\leq 2 K_d$, and the protein concentration was set such that 50–80% of fluorescent ligand is bound. The dissociation constant of a competing ligand was calculated with the correction to Cheng–Prusoff equation introduced by Nicolovska-Coleska and colleagues.²⁵ Assuming a one-site competitive-binding model, the equation used to calculate K_i values from IC_{50} values recovered from fitting data using Prism is

$$K_i = \frac{[I_{50}]}{\left(\frac{[L_{50}]}{K_d} + \frac{[P_0]}{K_d} + 1 \right)}$$

where $[I_{50}]$ is the concentration of free inhibitor at 50% inhibition, $[L_{50}]$, the concentration of free labeled ligand at 50% inhibition, and $[P_0]$, the concentration of free protein at 0% inhibition. Note that K_d for each protein–probe pair is the limit of resolvable K_i in a competition assay.

Protein Crystallization, X-ray Diffraction Data Collection, and Structure Determination. Purified BRD4-BrD1 protein (14 mg/mL) was mixed with a diazobenzene BrD inhibitor at a 1:10 molar ratio of protein/ligand. The complex was crystallized using the sitting-drop vapor-diffusion method at 20 $^{\circ}$ C by mixing 1 μ L of protein

solution with 1 μ L of the reservoir solution containing 15–30% PEG 4000, 0.2 M $MgCl_2$, and 0.1 M Tris-HCl, pH 8.5. Crystals were soaked in the corresponding mother liquor supplemented with 20% ethylene glycerol as a cryoprotectant before freezing in liquid nitrogen. X-ray diffraction data were collected at 100 K at beamline X6A of the National Synchrotron Light Source (NSLS) at Brookhaven National Laboratory. Data were processed using the HKL-2000 suite.²⁶ The BRD4-BD1 structure was solved by molecular replacement using the program MOLREP,²⁷ and the structure refinement was done using the program Refmac.²⁸ Graphics program COOT²⁹ was used for model building and visualization. Crystal diffraction data and refinement statistics for the structure are displayed in Table S2 (Supporting Information).

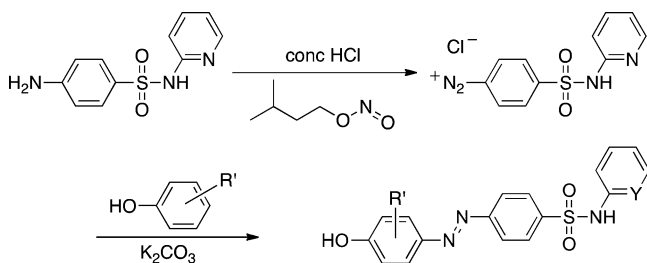
Cell Viability Study of Murine Macrophage Cells. Murine macrophage RAW264.7 cells were plated at a density of 1×10^4 cells per well in a 96-well plate and incubated at 37 $^{\circ}$ C for 18 h. The cells were then treated with the diazobenzene bromodomain inhibitors up to 100 μ M for 24 h. At the end of the 24 h incubation, 10 μ L of the MTT solution (4 mg/mL) was added to each well, and the plates were incubated at 37 $^{\circ}$ C for 4 h. The supernatants were then removed, and the cells were solubilized in 100 μ L of 100% DMSO. The diazobenzene compounds were first dissolved in DMSO and then diluted with culture medium to concentrations that ranged from 0.28 to 50 000 nM. The final concentration of DMSO was adjusted to 0.05% (v/v). The extent of the reduction was measured by the absorbance at 570/630 nm using an EnVision 2104 multilabel reader (PerkinElmer, Inc., Waltham, MA).

Assessing LPS-Induced IL-6 and Nitric Oxide Levels in Murine Macrophage Cells. Murine macrophage RAW264.7 cells were cultivated in DMEM (HyClone, Logan, UT) supplemented with 10% FBS (HyClone) at 37 $^{\circ}$ C in a humidified atmosphere of 5% CO_2 . Cells in 96-well plates (0.1 mL, 3×10^5 cells/mL) were treated with lead diazobenzene inhibitors. After 30 min, all supernatants were removed, and the cells were treated with LPS (1 μ g/mL) (Sigma-Aldrich Chemical Co., St. Louis, MO) and lead diazobenzene inhibitors. After 24 h, the supernatant was collected and measured using a mouse IL-6 ELISA assay kit (Thermo Scientific, Pittsburgh, PA). The lead diazobenzene bromodomain inhibitors were first dissolved in DMSO (Sigma-Aldrich Chemical Co.) and then diluted with culture medium to concentrations that ranged from 0.28 to 50 000 nM. The final concentration of DMSO was adjusted to 0.05% (v/v).

v). The assay was measured by an absorption reading at 570 nm using an EnVison 2104 multilabel reader (PerkinElmer, Inc.). For assessing LPS-induced nitric oxide release, nitrite production was measured by spectrophotometry at 520 nm using an EnVison 2104 multilabel reader (PerkinElmer, Inc.). Each experiment was performed in triplicate and plotted using Prism 5.0 (GraphPad Software, Inc.). The curve-fitting equation used was $\log(\text{inhibitor})$ versus response – variable slope (four parameters).

Chemical Synthesis. The core of the diazobenzene compounds was constructed by azo coupling³⁰ of the diazonium chloride intermediate **2** with appropriately functionalized phenol (Scheme 1).³¹ For C ring diazo analogues, 4-aminobenzenesulfonyl chloride precursors were first coupled to functionalized aromatic amines. The protective groups of the aromatic amines were either unmasked by sodium hydroxide aqueous solution or reduced with iron in ammonium chloride aqueous solution. Key intermediate **A** was accessed by treating the anilines with glacial acetic acid and isoamyl nitrite sequentially. Subsequent azo coupling with 2,6-dimethylphenol in the presence of potassium carbonate gave a variety of C ring diazobenzene analogues. A ring diazobenzene analogues were accessed through a simpler procedure. Sulfapyridine was treated with concentrated hydrogen chloride, and the resulting diazonium chloride reacted readily with various phenols under basic conditions to give diversified A ring diazobenzene analogues (Scheme 2).

Scheme 2. General Synthesis of a Ring Analogues of Diazobenzene



All nonaqueous reactions were carried out in oven-dried glassware under an atmosphere of argon. All solvents were purchased in anhydrous from Acros Organics and used without further purification. Automatic chromatography was performed on a Biotage Isolera system equipped with a variable wavelength detector and a fraction collector using a Biotage SNAP cartridge KP-Sil 10 g. Analytical thin-layer chromatography (TLC) was performed employing Sigma-Aldrich 250 μm 60F-254 silica plates. The plates were visualized either by exposure to UV light, staining with iodine-impregnated silica gel, or staining with ceric ammonium molybdate (CAM). Preparative TLC was performed employing Silicycle 1000 μm SiliaPlate Prep silica plates. LCMS analysis was conducted on an Agilent Technologies G1969A high-resolution API-TOF mass spectrometer attached to an Agilent Technologies 1200 HPLC system. Samples were ionized by electrospray ionization (ESI) in positive mode. Chromatography was performed on a 2.1 \times 150 mm Zorbax 300SB-C18 5 μm column with water containing 0.1% formic acid as solvent A and acetonitrile containing 0.1% formic acid as solvent B at a flow rate of 0.4 mL/min. The gradient program was as follows: 1% B (0–1 min), 1–99% B (1–4 min), and 99% B (4–8 min). The temperature of the column was held at 50 $^{\circ}\text{C}$ for the entire analysis. NMR spectra were acquired on a Bruker DRX-600 spectrometer at 600 MHz for ^1H and 150 MHz for ^{13}C . Chemical shifts are expressed in parts per million downfield from tetramethylsilane (TMS) using either TMS or the solvent resonance as an internal standard (TMS, ^1H : 0 ppm; chloroform, ^{13}C : 77.0 ppm; DMSO- d_6 , ^1H : 2.50 ppm; ^{13}C : 39.5 ppm; methanol- d_4 , ^1H : 3.31 ppm; ^{13}C : 49.0 ppm). Data are reported as follows: chemical shift, multiplicity (s = singlet, d = doublet, t = triplet, q = quartet, m = multiplet, and br = broad), integration, and coupling constant. IR spectra were obtained on a Bruker TENSOR 27 series FT-IR spectrometer equipped with a Diamond ATR. Melting point was

measured on an OptiMelt automatic melting point system MPA100 from Stanford Research System.

General Experimental Procedures. (E)-5-((2-Amino-4-hydroxy-5-methylphenyl)diazonyl)-2,4-dimethylbenzenesulfonic acid (**1**). A 100 mL round-bottomed flask was charged with concentrated HCl (5 mL) and crushed ice (1 g) and cooled to 0 $^{\circ}\text{C}$. To this flask were added 5-amino-2,4-xylene-sulfonic acid (230 mg, 1.15 mmol, 1.0 equiv) and NaNO_2 (1 N, 1 mL, 1.15 mmol, 1 equiv). The mixture was stirred at 0 $^{\circ}\text{C}$ for 2 h. 5-Amino-2-methylphenol (155 mg, 1.26 mmol, 1.2 equiv) was dissolved in a 10% NaOH(aq) solution (20 mL, 50 equiv). The previously prepared yellow color diazonium ion was added dropwise under argon over 10 min. The pH of the solution was maintained between 8 and 10 with the addition of small amount of 10% NaOH(aq). The solution was allowed to stir at 0 $^{\circ}\text{C}$ for 1 h and was quenched with 1 N HCl and adjusted to pH 7. Filtration provided the product as a fine red powder (335 mg, 95%). ^1H NMR (600 MHz, DMSO- d_6) δ 10.20 (br s, 1H), 7.97 (s, 1H), 7.48 (s, 1H), 7.11 (s, 1H), 6.41 (s, 1H), 2.51 (s, 3H), 2.48 (s, 3H), 2.07 (s, 3H). ^{13}C NMR (150 MHz, MeOD- d_4) δ 155.5, 148.0, 144.2, 141.5, 139.4, 139.2, 138.6, 134.0, 119.3, 117.5, 116.8, 114.4, 19.6, 16.0, 15.9. MS (m/z): calcd for $\text{C}_{15}\text{H}_{18}\text{N}_3\text{O}_4\text{S}^+ [\text{M} + \text{H}]^+$, 336.10; found, 336.10. Purity >95%, $t_{\text{R}} = 4.4$ min.

(E)-5-(3,5-Dimethyl-4-hydroxyphenylazo)-2,4-dimethylbenzenesulfonic acid (**2**). Following a similar procedure as compound **1**, compound **2** was obtained as a yellowish solid (74%). ^1H NMR (600 MHz, MeOD- d_4) δ 8.33 (s, 1H), 7.71 (s, 2H), 7.40 (s, 1H), 2.84 (s, 3H), 2.82 (s, 3H), 2.45 (s, 6H). ^{13}C NMR (150 MHz, MeOD- d_4) δ 151.1, 143.4, 137.7, 135.1, 133.7, 132.6, 130.4, 129.5, 110.5, 108.5, 29.3, 22.6, 21.1. MS (m/z): calcd for $\text{C}_{16}\text{H}_{19}\text{N}_2\text{O}_4\text{S}^+ [\text{M} + \text{H}]^+$, 335.11; found, 335.13.

(E)-3-((4-Hydroxy-3,5-dimethylphenyl)diazonyl)-N-(pyridin-2-yl)benzenesulfonamide (**3**). A 250 mL round-bottomed flask was charged with 4-nitrobenzenesulfonyl chloride (500.0 mg, 2.26 mmol, 1.0 equiv) dissolved in DCM (40 mL). The solution was cooled to 0 $^{\circ}\text{C}$. 2-Aminopyridine (212 mg, 2.26 mmol, 1.0 equiv) was dissolved in DCM (5 mL) and added carefully at 0 $^{\circ}\text{C}$ dropwise over 20 min. After 1 h, the solution was gradually warmed to rt and stirred overnight. The reaction was quenched by water (30.0 mL). The organic layer was washed sequentially with water and brine and dried over MgSO_4 . The volatiles were removed under reduced pressure. The crude product was recrystallized in a mixture of DCM and MeOH. Pure product **A** appeared as a pale-yellow powder (410.0 mg, 65%). A 100 mL pressure tube was charged with compound **A** (410.0 mg, 1.47 mmol, 1.0 equiv) and was dissolved in a 1:1 (v/v) MeOH/ H_2O mixture (20 mL). To this mixture were added iron (240 mg, 4.33 mmol, 2.95 equiv) and NH_4Cl (aq) (400 mg, 7.34 mmol, 5.0 equiv). The mixture was heated at 70 $^{\circ}\text{C}$ for 4 h. The reaction mixture was cooled and filtered through a Celite pad to remove the inorganic residues. The pad was washed (10 mL \times 3) with acetone. The combined filtrate was concentrated in vacuo. DI water (40 mL) was added, and the pH was adjusted to basic by the addition of NaHCO_3 . The solid was filtered and dried. Pure product **B** appeared as gray powder (250 mg, 68%). A 100 mL round-bottomed flask was charged with **B** (100.0 mg, 0.41 mmol, 1.0 equiv) and concentrated HCl (0.16 mL, 0.41 mmol, 1.0 equiv). The mixture was dissolved in a MeOH/ACN mixture 1.5 mL/1.5 mL. The reaction solution was stirred at 0 $^{\circ}\text{C}$ for 15 min. Isoamyl nitrite (55 μL , 0.41 mmol, 1.0 equiv) was added dropwise under argon over 15 min. The bright-yellow solution was stirred at 0 $^{\circ}\text{C}$ for 1 h and gradually warmed to rt for 1 h. 2,6-Dimethylphenol (50.0 mg, 0.41 mmol, 1.0 equiv) and K_2CO_3 (280.6 mg, 2.03 mmol, 5.0 equiv) were premixed and deoxygenized by argon for 15 min. The previously prepared amber color diazonium ion **C** was added dropwise under argon. At the end of the addition, the pH of the solution was maintained between 8 and 10 using K_2CO_3 . The solution was stirred at 0 $^{\circ}\text{C}$ for 1 h and then at rt overnight. The resultant solution was adjusted to pH 1. The solid was filtered and dried. Pure product **3** appeared as an orange powder (134.1 mg, 86%). ^1H NMR (600 MHz, DMSO- d_6) δ 9.29 (br s, 1H), 8.18 (s, 1H), 7.98 (d, $J = 7.8$ Hz, 1H), 7.97–7.92 (m, 2H), 7.76 (dt, $J = 8.4, 1.5$ Hz, 1H), 7.70 (t, $J = 7.8$ Hz, 1H), 7.59 (s, 2H), 7.20 (d, $J = 9.0$ Hz, 1H), 6.84 (t, $J = 6.0$ Hz, 1H),

2.24 (s, 6H). ^{13}C NMR (150 MHz, DMSO- d_6) δ 160.9, 156.8, 155.2, 148.0, 146.9, 144.5, 133.5, 131.4, 130.8, 129.8, 128.3, 127.0, 122.3, 121.4, 117.7, 19.9. MS (m/z): calcd for $\text{C}_{19}\text{H}_{19}\text{N}_4\text{O}_3\text{S}^+$ [$\text{M} + \text{H}$] $^+$, 383.11; found, 383.11. Purity >99%, t_{R} = 5.0 min.

(*E*)-4-((4-Hydroxy-3,5-dimethylphenyl)diazanyl)-*N*-(pyridin-2-yl)-benzenesulfonamide (**4**, MS435). Following a similar procedure as compound **3**, compound **4** was prepared as an orange powder (80%). ^1H NMR (600 MHz, DMSO- d_6) δ 12.2 (br s, 1H), 9.33 (br s, 1H), 8.00 (d, J = 8.4 Hz, 1H), 7.98–7.93 (m, 2H), 7.87 (d, J = 8.4 Hz, 2H), 7.74 (t, J = 8.4 Hz, 1H), 7.57 (s, 2H), 7.20 (d, J = 9.0 Hz, 1H), 6.85 (t, J = 6.6 Hz, 1H), 2.14 (s, 6H). ^{13}C NMR (150 MHz, DMSO- d_6) δ 158.3, 154.3, 154.0, 145.4, 143.7, 141.8, 141.6, 128.6, 125.6, 124.3, 122.8, 120.0, 114.8, 17.1. MS (m/z): calcd for $\text{C}_{19}\text{H}_{19}\text{N}_4\text{O}_3\text{S}^+$ [$\text{M} + \text{H}$] $^+$, 383.11; found, 383.11. Purity >99%, t_{R} = 2.1 min. (Chromatography was performed on a 2.1×50 mm Acquity BEH C-18 column using acetonitrile as solvent A and water containing 0.025% TFA as solvent B at a flow rate of 0.5 mL/min. The gradient program was as follows: 90% B (0–0.5 min), 90–10% B (0.5–3 min), and 10% B (3–6 min).)

(*E*)-4-((4-Hydroxy-3,5-dimethylphenyl)diazanyl)-*N*-(4-(trifluoromethyl)benzyl)benzenesulfonamide (**5**). ^1H NMR (600 MHz, MeOD- d_4) δ 7.93 (d, J = 8.4 Hz, 2H), 7.89 (d, J = 8.4 Hz, 2H), 7.62 (s, 2H), 7.54 (d, J = 8.4 Hz, 2H), 7.44 (d, J = 8.4 Hz, 2H), 4.20 (s, 2H), 2.30 (s, 6H). ^{13}C NMR (150 MHz, MeOD- d_4) δ 160.5, 157.7, 148.6, 144.7, 144.0, 132.1, 131.9, 130.8, 130.5, 127.9, 127.6 (d), 126.6, 125.1, 48.7, 18.1. IR (neat): ν 3498 (–OH), 3247 (–NH–), 1616 (–C=N–), 1591 (–N=N–), 1382 (–SO $_2$ –). MS (m/z): calcd for $\text{C}_{22}\text{H}_{21}\text{F}_3\text{N}_3\text{O}_3\text{S}^+$ [$\text{M} + \text{H}$] $^+$, 464.12; found, 464.12. Purity >99%, t_{R} = 6.5 min. mp 195.7 $^{\circ}\text{C}$.

The following compounds were synthesized following Scheme 1.

(*E*)-4-((4-Hydroxy-3,5-dimethylphenyl)diazanyl)-*N*-methyl-*N*-(pyridin-2-yl)benzenesulfonamide (**6**). ^1H NMR (600 MHz, MeOD- d_4) δ 8.16–8.12 (m, 1H), 8.10 (d, J = 8.4 Hz, 2H), 7.67 (d, J = 8.4 Hz, 2H), 7.63 (s, 2H), 7.04 (t, J = 6.6 Hz, 1H), 6.86 (d, J = 7.2 Hz, 1H), 6.63 (t, J = 7.2 Hz, 1H), 2.30 (s, 6H), 2.18 (s, 3H). ^{13}C NMR (150 MHz, DMSO- d_6) δ 161.1, 156.9, 155.6, 148.3, 146.7, 143.1, 140.9, 130.7, 127.8, 126.8, 122.1, 115.1, 114.1, 31.5, 18.1. MS (m/z): calcd for $\text{C}_{20}\text{H}_{21}\text{N}_4\text{O}_3\text{S}^+$ [$\text{M} + \text{H}$] $^+$, 397.13; found, 397.13. Yield: 31%, purity >99%, t_{R} = 4.8 min.

(*E*)-4-((4-Hydroxy-3,5-dimethylphenyl)diazanyl)-*N*-(3-(trifluoromethyl)phenyl)benzenesulfonamide (**7**). ^1H NMR (600 MHz, CDCl $_3$) δ 7.90 (m, 4H), 7.65 (s, 2H), 7.38 (m, 3H), 7.29 (br s, 1H), 6.82 (s, 1H), 5.10 (s, 1H), 2.34 (s, 6H). MS (m/z): calcd for $\text{C}_{21}\text{H}_{19}\text{F}_3\text{N}_3\text{O}_3\text{S}^+$ [$\text{M} + \text{H}$] $^+$, 450.11; found, 450.11. Yield: 68%, purity >99%, t_{R} = 6.5 min.

(*E*)-*N*-(4-Chloropyridin-2-yl)-4-((4-hydroxy-3,5-dimethylphenyl)diazanyl)benzenesulfonamide (**8**). ^1H NMR (600 MHz, DMSO- d_6) δ 9.39 (br s, 1H), 8.18 (d, J = 1.8 Hz, 1H), 8.04 (d, J = 7.8 Hz, 2H), 7.89 (d, J = 7.8 Hz, 2H), 7.79 (dd, J = 9.0, 1.8 Hz, 1H), 7.56 (s, 2H), 7.08 (d, J = 9.0 Hz, 1H), 7.01 (d, J = 5.6 Hz, 1H), 2.23 (s, 6H). ^{13}C NMR (150 MHz, DMSO- d_6) δ 161.2, 157.7, 153.2, 149.3, 148.2, 143.9, 141.7, 131.8, 128.3, 127.1, 125.6, 121.8, 116.7, 19.8. MS (m/z): calcd for $\text{C}_{19}\text{H}_{18}\text{ClN}_4\text{O}_3\text{S}^+$ [$\text{M} + \text{H}$] $^+$, 417.08; found, 417.08. Yield: 87%, purity >99%, t_{R} = 5.3 min.

(*E*)-6-(4-((4-Hydroxy-3,5-dimethylphenyl)diazanyl)phenylsulfonamido)nicotinic Acid (**9**). ^1H NMR (600 MHz, DMSO- d_6) δ 9.31 (br s, 1H), 8.24–8.14 (m, 2H), 8.03 (d, J = 8.4 Hz, 2H), 7.88 (d, J = 8.4 Hz, 2H), 7.72 (s, 1H), 7.57 (s, 2H), 7.50 (s, 1H), 7.27 (d, J = 4.8 Hz, 2H), 2.24 (s, 6H). ^{13}C NMR (150 MHz, MeOD- d_4) δ 169.0, 161.2, 157.3, 156.1, 148.1, 145.0, 131.4, 128.4, 127.1, 125.5, 122.3, 117.7, 114.8, 19.9. MS (m/z): calcd for $\text{C}_{20}\text{H}_{18}\text{N}_4\text{O}_5\text{S}^+$ [M] $^+$, 426.11; found, 426.11. Yield: 24%, purity >99%, t_{R} = 5.1 min.

(*E*)-*N*-(5-Chloropyridin-2-yl)-4-((4-hydroxy-3,5-dimethylphenyl)diazanyl)benzenesulfonamide (**10**). ^1H NMR (600 MHz, DMSO- d_6) δ 9.36 (br s, 1H), 8.03 (d, J = 7.8 Hz, 4H), 7.89 (d, J = 7.8 Hz, 2H), 7.57 (s, 2H), 7.16 (s, 1H), 7.01 (d, J = 5.6 Hz, 1H), 2.24 (s, 6H). ^{13}C NMR (150 MHz, DMSO- d_6) δ 161.1, 157.4, 156.6, 149.2, 148.2, 145.1, 131.7, 131.3, 128.3, 127.1, 125.6, 119.9, 115.8, 19.8. MS (m/z): calcd for $\text{C}_{19}\text{H}_{18}\text{ClN}_4\text{O}_3\text{S}^+$ [$\text{M} + \text{H}$] $^+$, 417.08; found, 417.07. Yield: 87%, purity >99%, t_{R} = 5.3 min.

(*E*)-*N*-(5-Bromopyridin-2-yl)-4-((4-hydroxy-3,5-dimethylphenyl)diazanyl)benzenesulfonamide (**11**). ^1H NMR (600 MHz, MeOD- d_4) δ 7.89–7.80 (m, 4H), 7.58 (s, 2H), 7.36 (d, J = 8.4 Hz, 2H), 7.04 (d, J = 8.4 Hz, 2H), 2.27 (s, 6H). ^{13}C NMR (150 MHz, MeOD- d_4) δ 160.6, 157.9, 148.5, 142.6, 139.6, 134.6, 130.7, 127.5, 126.6, 125.5, 125.0, 120.2, 18.1. MS (m/z): calcd for $\text{C}_{19}\text{H}_{18}\text{BrN}_4\text{O}_3\text{S}^+$ [$\text{M} + \text{H}$] $^+$, 462.03; found, 462.00. Yield: 55%, purity >99%, t_{R} = 5.6 min.

(*E*)-4-((4-Hydroxy-3,5-dimethylphenyl)diazanyl)-*N*-(5-methoxy-pyridin-2-yl)benzenesulfonamide (**12**). ^1H NMR (600 MHz, DMSO- d_6) δ 10.85 (s, 1H), 9.35 (s, 1H), 7.99 (d, J = 8.4 Hz, 2H), 7.92–7.85 (m, 3H), 7.59 (s, 2H), 7.37 (m, 1H), 7.11 (m, 1H), 3.73 (s, 3H), 2.26 (s, 6H). MS (m/z): calcd for $\text{C}_{20}\text{H}_{21}\text{N}_4\text{O}_4\text{S}^+$ [$\text{M} + \text{H}$] $^+$, 413.13; found, 413.12. Yield: 57%, purity >99%, t_{R} = 6.2 min.

(*E*)-4-((4-Hydroxy-3,5-dimethylphenyl)diazanyl)-*N*-(4-methoxyphenyl)benzenesulfonamide (**13**). ^1H NMR (600 MHz, CDCl $_3$) δ 7.86 (d, J = 8.4 Hz, 2H), 7.79 (d, J = 8.4 Hz, 2H), 7.65 (s, 2H), 6.98 (d, J = 9.0 Hz, 2H), 6.77 (d, J = 9.0 Hz, 1H), 6.28 (s, 1H), 5.10 (s, 1H), 3.76 (s, 3H), 2.34 (s, 6H). MS (m/z): calcd for $\text{C}_{21}\text{H}_{22}\text{N}_3\text{O}_4\text{S}^+$ [$\text{M} + \text{H}$] $^+$, 412.13; found, 412.13. Yield: 57%, purity >99%, t_{R} = 6.3 min.

(*E*)-4-((4-Hydroxy-3,5-dimethylphenyl)diazanyl)-*N*-(4-(trifluoromethyl)phenyl)benzenesulfonamide (**14**). ^1H NMR (600 MHz, DMSO- d_6) δ 11.02 (s, 1H), 9.38 (s, 1H), 7.98 (d, J = 8.4 Hz, 2H), 7.92 (d, J = 8.4 Hz, 2H), 7.63 (d, J = 8.4 Hz, 2H), 7.59 (s, 2H), 7.31 (d, J = 8.4 Hz, 2H), 2.26 (s, 6H). MS (m/z): calcd for $\text{C}_{21}\text{H}_{19}\text{F}_3\text{N}_3\text{O}_3\text{S}^+$ [$\text{M} + \text{H}$] $^+$, 450.11; found, 450.13. Purity >95%, t_{R} = 6.5 min.

(*E*)-4-((4-Hydroxy-3,5-dimethylphenyl)diazanyl)-phenylsulfonamido)benzamide (**15**). ^1H NMR (600 MHz, DMSO- d_6) δ 10.81 (br s, 1H), 8.36 (d, J = 8.4 Hz, 1H), 8.05 (d, J = 8.4 Hz, 1H), 8.00 (d, J = 8.4 Hz, 1H), 7.92 (d, J = 8.4 Hz, 1H), 7.84–7.77 (m, 2H), 7.75–7.66 (m, 2H), 7.28–7.20 (m, 2H), 7.14 (d, J = 8.4 Hz, 2H), 2.48 (s, 6H). ^{13}C NMR (150 MHz, DMSO- d_6) δ 170.3, 160.0, 153.0, 149.5, 143.5, 142.6, 132.8, 132.0, 131.3, 130.9, 128.6, 126.8, 122.1, 121.8, 16.5. MS (m/z): calcd for $\text{C}_{21}\text{H}_{21}\text{N}_4\text{O}_4\text{S}^+$ [$\text{M} + \text{H}$] $^+$, 425.13; found, 425.14. Yield: 24%, purity >99%, t_{R} = 5.4 min.

(*E*)-*N*-(5-Fluoropyridin-2-yl)-4-((4-hydroxy-3,5-dimethylphenyl)diazanyl)benzenesulfonamide (**16**). ^1H NMR (600 MHz, DMSO- d_6) δ 9.47 (br s, 1H), 8.15 (d, J = 2.4 Hz, 1H), 8.02 (d, J = 7.8 Hz, 2H), 7.88 (d, J = 7.8 Hz, 2H), 7.64 (dt, J = 7.8, 2.4 Hz, 1H), 7.56 (s, 2H), 7.11 (dd, J = 7.8, 2.4 Hz, 1H), 2.23 (s, 6H). ^{13}C NMR (150 MHz, DMSO- d_6) δ 161.2, 159.9, 158.3, 157.6, 150.9, 148.1, 144.0, 131.7, 129.4, 128.3, 127.1, 125.6, 117.1, 19.8. MS (m/z): calcd for $\text{C}_{19}\text{H}_{18}\text{FN}_4\text{O}_3\text{S}^+$ [$\text{M} + \text{H}$] $^+$, 401.11; found, 401.08. Yield: 78%, purity >99%, t_{R} = 5.3 min.

(*E*)-*N*-(4-Fluorophenyl)-4-((4-hydroxy-3,5-dimethylphenyl)diazanyl)benzenesulfonamide (**17**). ^1H NMR (600 MHz, CDCl $_3$) δ 10.31 (br s, 1H), 9.40 (br s, 1H), 8.00–7.79 (m, 4H), 7.59 (s, 2H), 7.21–7.07 (m, 4H), 2.25 (s, 6H). MS (m/z): calcd for $\text{C}_{20}\text{H}_{19}\text{FN}_3\text{O}_3\text{S}^+$ [$\text{M} + \text{H}$] $^+$, 400.11; found, 400.12. Yield: 76%, purity >99%, t_{R} = 6.4 min.

(*E*)-4-((4-Hydroxy-3,5-dimethylphenyl)diazanyl)-2-methoxy-*N*-(pyridin-2-yl)benzenesulfonamide (**18**). ^1H NMR (600 MHz, DMSO- d_6) δ 9.31 (br s, 1H), 8.00 (d, J = 8.4 Hz, 1H), 7.96 (d, J = 4.8 Hz, 1H), 7.70 (t, J = 7.8 Hz, 1H), 7.58 (s, 2H), 7.47–7.41 (m, 2H), 7.18 (d, J = 8.4 Hz, 1H), 6.85 (t, J = 6.6 Hz, 1H), 3.8 (s, 3H), 2.24 (s, 6H). ^{13}C NMR (150 MHz, DMSO- d_6) δ 160.6, 158.7, 156.6 (m), 148.0, 143.2, 140.9, 133.9, 131.4, 128.4, 127.1, 122.3, 117.5, 117.0, 114.9, 114.1, 31.5, 18.1. MS (m/z): calcd for $\text{C}_{20}\text{H}_{21}\text{N}_4\text{O}_5\text{S}^+$ [$\text{M} + \text{H}$] $^+$, 413.13; found, 413.13. Yield: 31%, purity >99%, t_{R} = 4.8 min.

The following compounds were synthesized following Scheme 2.

(*E*)-4-((3,5-Dichloro-4-hydroxyphenyl)diazanyl)-*N*-(pyridin-2-yl)benzenesulfonamide (**19**). ^1H NMR (600 MHz, MeOD- d_4) δ 8.08 (d, J = 8.4 Hz, 1H), 8.02–7.94 (m, 3H), 7.93 (s, 2H), 7.74 (t, J = 7.8 Hz, 2H), 7.30 (d, J = 9.0 Hz, 1H), 6.89 (t, J = 6.6 Hz, 1H). ^{13}C NMR (150 MHz, DMSO- d_6) δ 158.0, 156.5, 156.0, 146.7, 146.5, 142.9, 142.5, 131.3, 131.0, 126.8 (m), 125.9, 118.1, 115.7. MS (m/z): calcd for $\text{C}_{17}\text{H}_{13}\text{Cl}_2\text{N}_4\text{O}_3\text{S}^+$ [$\text{M} + \text{H}$] $^+$, 423.01, 425.01; found, 423.01, 425.01. Yield: 75%, purity >95%, t_{R} = 5.9 min.

(*E*)-4-((3-Bromo-4-hydroxy-5-methylphenyl)diazanyl)-*N*-(pyridin-2-yl)benzenesulfonamide (**20**). ^1H NMR (600 MHz, DMSO- d_6) δ

10.12 (s, 1H), 8.13–7.98 (m, 3H), 7.97–7.87 (m, 3H), 7.83–7.72 (m, 2H), 7.35–7.10 (m, 1H), 6.95–6.75 (m, 1H), 2.34 (s, 3H). ^{13}C NMR (150 MHz, DMSO- d_6) δ 158.9, 157.8, 156.6, 153.9, 148.6, 147.2, 144.5, 132.6, 131.0, 130.9, 130.3, 128.3, 125.8, 124.9, 124.5, 123.4, 117.7, 115.8, 20.1. MS (m/z): calcd for $\text{C}_{18}\text{H}_{16}\text{BrN}_4\text{O}_3\text{S}^+$ [$\text{M} + \text{H}$] $^+$, 447.01 and 449.01; found, 446.99, 448.98. Yield: 94%, purity >99%, t_{R} = 6.0 min.

(*E*)-4-((3-Chloro-4-hydroxy-5-methylphenyl)diazenyl)-*N*-(pyridin-2-yl)benzenesulfonamide (**21**). ^1H NMR (600 MHz, DMSO- d_6) δ 10.22 (s, 1H), 9.08 (s, 1H), 8.02 (d, J = 8.4 Hz, 2H), 8.00–7.94 (m, 1H), 7.91 (d, J = 8.4 Hz, 2H), 7.79–7.68 (m, 3H), 7.21 (d, J = 8.4 Hz, 1H), 6.85 (t, J = 6.6 Hz, 1H), 2.30 (s, 3H). ^{13}C NMR (150 MHz, DMSO- d_6) δ 157.9, 156.6, 153.9, 148.1, 147.2, 144.4, 132.6, 131.0, 130.9, 130.3, 128.3, 125.8, 124.9, 124.5, 123.4, 117.7, 115.8, 20.1. MS (m/z): calcd for $\text{C}_{18}\text{H}_{16}\text{ClN}_4\text{O}_3\text{S}^+$ [$\text{M} + \text{H}$] $^+$, 403.06; found, 403.05. Purity >99%, t_{R} = 6.0 min.

(*E*)-4-((3-Bromo-4-hydroxyphenyl)diazenyl)-*N*-(pyridin-2-yl)benzenesulfonamide (**22**). ^1H NMR (600 MHz, DMSO- d_6) δ 8.10 (s, 1H), 8.00–7.93 (m, 1H), 7.92 (d, J = 8.4 Hz, 2H), 7.82 (d, J = 9.0 Hz, 1H), 7.73 (t, J = 7.2 Hz, 2H), 7.29 (d, J = 8.4 Hz, 1H), 7.00 (d, J = 9.0 Hz, 1H), 6.88 (t, J = 6.0 Hz, 1H). ^{13}C NMR (150 MHz, MeOD- d_4) δ 158.8, 154.1, 153.9, 145.8, 144.2, 141.7, 128.3, 126.9, 126.3, 123.1, 117.0, 114.9 (br), 111.2. MS (m/z): calcd for $\text{C}_{17}\text{H}_{14}\text{BrN}_4\text{O}_3\text{S}^+$ [$\text{M} + \text{H}$] $^+$, 432.99 and 434.99; found, 432.99 and 434.99. Yield: 80%, purity >95%, t_{R} = 5.9 min.

(*E*)-4-((3-Chloro-4-hydroxyphenyl)diazenyl)-*N*-(pyridin-2-yl)benzenesulfonamide (**23**). ^1H NMR (600 MHz, DMSO- d_6) δ 11.34 (s, 1H), 8.09 (d, J = 8.4 Hz, 1H), 8.03 (d, J = 7.8 Hz, 2H), 7.95–7.89 (m, 3H), 7.87–7.81 (m, 2H), 7.77 (m, 1H), 7.24 (d, J = 9.0 Hz, 1H), 7.20 (d, J = 9.0 Hz, 1H), 6.86 (s, 1H). MS (m/z): calcd for $\text{C}_{17}\text{H}_{14}\text{ClN}_4\text{O}_3\text{S}^+$ [$\text{M} + \text{H}$] $^+$, 389.05; found, 389.05. Yield: 100%, purity >99%, t_{R} = 5.9 min.

(*E*)-4-((4-Hydroxy-3-methylphenyl)diazenyl)-*N*-(pyridin-2-yl)benzenesulfonamide (**24**). ^1H NMR (600 MHz, MeOD- d_4) δ 8.05 (d, J = 8.4 Hz, 2H), 7.95 (d, J = 5.3 Hz, 1H), 7.89 (d, J = 8.4 Hz, 2H), 7.77–7.70 (m, 2H), 7.68 (d, J = 8.4 Hz, 1H), 7.29 (d, J = 8.7 Hz, 1H), 6.94–6.87 (m, 2H), 2.26 (s, 3H). ^{13}C NMR (150 MHz, DMSO- d_6) δ 162.0, 156.6, 155.9, 147.9, 144.9, 144.0, 143.0, 129.9, 127.5, 127.3, 125.7, 124.3, 117.4, 116.8, 116.7, 17.3. IR (neat): ν 3326 (–OH), 1641 (–C=N–), 1593 (–N=N–), 1396 (–SO $_2$ –). MS (m/z): calcd for $\text{C}_{18}\text{H}_{17}\text{N}_4\text{O}_3\text{S}^+$ [$\text{M} + \text{H}$] $^+$, 369.10; found, 369.11. Purity >99%, t_{R} = 5.7 min. mp 248.1 °C.

(*E*)-4-((3,5-Dibromo-4-hydroxyphenyl)diazenyl)-*N*-(pyridin-2-yl)benzenesulfonamide (**25**). ^1H NMR (600 MHz, MeOD- d_4) δ 8.12 (s, 1H), 8.08 (d, J = 8.4 Hz, 2H), 8.00–7.92 (m, 4H), 7.74 (t, J = 7.8 Hz, 2H), 7.30 (d, J = 9.0 Hz, 2H), 6.85 (t, J = 6.6 Hz, 1H). ^{13}C NMR (150 MHz, DMSO- d_6) δ 169.6, 157.8, 157.2, 146.1, 143.0, 141.3, 140.8, 139.8, 131.3, 130.7, 130.4, 126.2, 124.0, 117.9, 115.5. MS (m/z): calcd for $\text{C}_{17}\text{H}_{13}\text{Br}_2\text{N}_4\text{O}_3\text{S}^+$ [$\text{M} + \text{H}$] $^+$, 510.90, 512.90, 514.90; found, 510.90, 512.90, 514.90. Yield: 47%, purity >99%, t_{R} = 6.0 min.

(*E*)-4-((4-Hydroxy-3-(trifluoromethyl)phenyl)diazenyl)-*N*-(pyridin-2-yl)benzenesulfonamide (**26**). ^1H NMR (600 MHz, MeOD- d_4) δ 8.17–8.13 (m, 1H), 8.08 (d, J = 9.0 Hz, 2H), 8.05 (d, J = 8.4 Hz, 1H), 8.03–7.95 (m, 3H), 7.74 (t, J = 7.8 Hz, 1H), 7.30 (d, J = 8.4 Hz, 2H), 7.09 (d, J = 9.0 Hz, 1H), 6.88 (t, J = 6.6 Hz, 1H). MS (m/z): calcd for $\text{C}_{18}\text{H}_{14}\text{F}_3\text{N}_4\text{O}_3\text{S}^+$ [$\text{M} + \text{H}$] $^+$, 423.07; found, 423.08. Yield: 39%, purity >99%, t_{R} = 5.8 min.

(*E*)-4-((2-Amino-4-hydroxy-5-methylphenyl)diazenyl)-*N*-(pyridin-2-yl)benzenesulfonamide (**27**, MS3436). ^1H NMR (600 MHz, DMSO- d_6) δ 10.28 (br s, 1H), 7.98 (m, 1H), 7.90 (d, J = 8.4 Hz, 2H), 7.82 (d, J = 8.4 Hz, 2H), 7.71 (t, J = 7.2 Hz, 2H), 7.37 (s, 1H), 7.17 (d, J = 8.4 Hz, 1H), 7.11 (br s, 2H), 6.85 (t, J = 6.0 Hz, 1H), 6.22 (s, 1H), 2.00 (s, 3H). ^{13}C NMR (150 MHz, DMSO- d_6) δ 162.0, 155.4, 153.7, 147.0, 141.0, 138.2, 133.2, 131.3, 128.7, 128.2, 121.9, 115.4, 114.4, 103.4, 100.4, 15.7. MS (m/z): calcd for $\text{C}_{18}\text{H}_{18}\text{N}_5\text{O}_3\text{S}^+$ [$\text{M} + \text{H}$] $^+$, 384.11; found, 384.12. Yield: 87%, purity >99%, t_{R} = 5.6 min.

(*E*)-4-((2-Amino-4-hydroxy-3,5-dimethylphenyl)diazenyl)-*N*-(pyridin-2-yl)benzenesulfonamide (**28**, MS267). ^1H NMR (600 MHz, DMSO- d_6) δ 8.01 (d, J = 4.8 Hz, 1H), 7.85 (d, J = 8.4 Hz, 2H), 7.76 (d, J = 8.4 Hz, 2H), 7.70 (t, J = 7.8 Hz, 1H), 7.46 (s, 1H), 7.15 (d, J = 7.8 Hz, 1H), 6.86 (t, J = 6.0 Hz, 1H), 3.90–3.70 (m, 4H), 2.00 (s,

3H), 1.89 (s, 3H). ^{13}C NMR (150 MHz, DMSO- d_6) δ 156.2, 154.9 (br), 153.0 (br), 146.8, 143.5, 140.1 (br), 134.7, 131.2, 122.9, 120.7, 119.0, 116.8, 116.4, 109.9, 19.9, 12.7. MS (m/z): calcd for $\text{C}_{19}\text{H}_{20}\text{N}_5\text{O}_3\text{S}^+$ [$\text{M} + \text{H}$] $^+$, 398.13; found, 398.12. Yield: 89%, purity >99%, t_{R} = 5.4 min.

(*E*)-4-((2-Amino-3-chloro-4-hydroxy-5-methylphenyl)diazenyl)-*N*-(pyridin-2-yl)benzenesulfonamide (**29**, MS363). A 50 mL round-bottomed flask was charged with sulfapyridine (100.0 mg, 0.40 mmol, 1.0 equiv) and concentrated HCl (87.5 mg, 160 μL , 2.40 mmol, 5.98 equiv). The mixture was dissolved in a MeOH/ACN mixture (3 mL/3 mL). The solution was cooled to 0 °C and stirred for 15 min. Isoamyl nitrite (47.0 mg, 54 μL , 0.40 mmol, 1.0 equiv) was added dropwise under argon over 10 min. The solution was stirred at 0 °C for 45 min. Meanwhile, to another 50 mL round-bottomed flask were added 3-amino-2-chloro-6-cresol (63.0 mg, 0.40 mmol, 1.0 equiv) and potassium carbonate (276.3 mg, 2.0 mmol, 5.0 equiv). To this mixture were added methanol (1.0 mL) and DI H $_2$ O (8.0 mL). The solution was deoxygenated for 15 min by argon. The resultant solution was cooled to 0 °C. The previously prepared amber color diazonium ion was added dropwise under argon over 15 min. At the end of the addition, the pH of the solution was maintained between 8 and 10. The solution was allowed to stir at 0 °C for 1 h and then quenched with 1 N HCl to reach pH 1. The product was filtered and dried under vacuum. The pure product appeared as a fine red powder (167.0 mg, 99%). ^1H NMR (600 MHz, DMSO- d_6) δ 11.51 (s, 1H), 8.04 (s, 1H), 7.97–7.78 (m, 3H), 7.78–7.62 (m, 3H), 7.53 (s, 1H), 7.15 (s, 1H), 6.89 (s, 1H), 6.73 (br s, 2H), 1.98 (s, 3H). ^{13}C NMR (150 MHz, DMSO- d_6) δ 158.1, 156.1, 155.4, 146.8, 146.3, 143.3, 142.0, 133.5, 132.0, 131.3, 130.6, 119.0, 116.7, 115.9, 115.7, 115.4, 107.4, 19.7. MS (m/z): calcd for $\text{C}_{18}\text{H}_{17}\text{ClN}_5\text{O}_3\text{S}^+$ [$\text{M} + \text{H}$] $^+$, 418.07; found, 418.08. Purity >99%, t_{R} = 5.5 min.

(*E*)-4-((2-Amino-4-hydroxy-5-methoxyphenyl)diazenyl)-*N*-(pyridin-2-yl)benzenesulfonamide (**30**). ^1H NMR (600 MHz, MeOD- d_4) δ 8.00 (d, J = 4.8 Hz, 1H), 7.88 (d, J = 8.4 Hz, 2H), 7.66 (dt, J = 7.2 Hz, 1.2, 2H), 7.55 (d, J = 8.4 Hz, 2H), 7.20–7.15 (m, 1H), 6.93 (t, J = 6.6 Hz, 1H), 6.89–6.84 (m, 2H), 6.76 (s, 1H), 3.84 (s, 3H). MS (m/z): calcd for $\text{C}_{18}\text{H}_{18}\text{N}_5\text{O}_4\text{S}^+$ [$\text{M} + \text{H}$] $^+$, 400.11; found, 400.11. Yield: 15%, purity >99%, t_{R} = 5.0 min.

(*E*)-4-((5-Hydroxy-4,6-dimethylpyridin-2-yl)diazenyl)-*N*-(pyridin-2-yl)benzenesulfonamide (**31**). ^1H NMR (600 MHz, MeOD- d_4) δ 8.11 (d, J = 8.5 Hz, 2H), 8.04 (d, J = 8.4 Hz, 2H), 7.94 (d, J = 5.3 Hz, 1H), 7.78–7.74 (m, 2H), 7.32 (d, J = 8.8 Hz, 1H), 6.89 (t, J = 6.4 Hz, 1H), 2.59 (s, 3H), 2.39 (s, 3H). HRMS (m/z): calcd for $\text{C}_{18}\text{H}_{18}\text{N}_5\text{O}_3\text{S}^+$ [$\text{M} + \text{H}$] $^+$, 384.113; found, 384.112. Purity >96%, t_{R} = 4.3 min.

(*E*)-4-((5-Hydroxy-3,4,6-trimethylpyridin-2-yl)diazenyl)-*N*-(pyridin-2-yl)benzenesulfonamide (**32**). ^1H NMR (600 MHz, MeOD- d_4) δ 8.11 (d, J = 8.2 Hz, 2H), 8.01 (d, J = 4.9 Hz, 2H), 7.94 (d, J = 5.3 Hz, 1H), 7.75 (t, J = 7.9 Hz, 1H), 7.31 (d, J = 8.8 Hz, 1H), 6.89 (t, J = 6.4 Hz, 1H), 2.70 (s, 3H), 2.62 (s, 3H), 2.38 (s, 3H). HRMS (m/z): calcd for $\text{C}_{19}\text{H}_{20}\text{N}_5\text{O}_3\text{S}^+$ [$\text{M} + \text{H}$] $^+$, 398.128; found, 398.127. Purity >90%, t_{R} = 4.7 min.

(*E*)-4-((3,4-Dihydroxy-5-methylphenyl)diazenyl)-*N*-(pyridin-2-yl)benzenesulfonamide (**33**). ^1H NMR (600 MHz, DMSO- d_6) δ 10.25 (s, 1H), 9.95 (s, 1H), 8.70 (s, 1H), 8.20–7.95 (m, 3H), 7.90 (d, J = 8.4 Hz, 2H), 7.82–7.70 (m, 2H), 7.30–7.13 (m, 2H), 6.98–6.80 (m, 1H), 2.22 (s, 3H). MS (m/z): calcd for $\text{C}_{18}\text{H}_{17}\text{N}_4\text{O}_4\text{S}^+$ [$\text{M} + \text{H}$] $^+$, 385.10; found, 389.05. Yield: 79%, purity >99%, t_{R} = 5.5 min.

(*E*)-4-((3,4-Dihydroxyphenyl)diazenyl)-*N*-(pyridin-2-yl)benzenesulfonamide (**34**). ^1H NMR (600 MHz, DMSO- d_6) δ 8.11–7.96 (m, 3H), 7.87 (d, J = 7.8 Hz, 2H), 7.77–7.70 (m, 2H), 7.39 (d, J = 8.4 Hz, 1H), 7.34 (s, 1H), 7.27–7.10 (m, 2H), 6.93 (d, J = 8.4 Hz, 1H), 6.91–6.80 (m, 2H). MS (m/z): calcd for $\text{C}_{17}\text{H}_{15}\text{N}_4\text{O}_4\text{S}^+$ [$\text{M} + \text{H}$] $^+$, 371.08; found, 371.10. Yield: 65%, purity >99%, t_{R} = 5.4 min.

(*E*)-4-((4-Hydroxy-3-methylphenyl)diazenyl)-*N*-(4-(trifluoromethyl)benzyl)benzenesulfonamide (**35**). ^1H NMR (600 MHz, MeOD- d_4) δ 7.94 (d, J = 8.4 Hz, 2H), 7.91 (d, J = 8.4 Hz, 2H), 7.76 (d, J = 1.9 Hz, 1H), 7.70 (dd, J = 7.8, 1.9 Hz, 1H), 7.54 (d, J = 8.4 Hz, 2H), 7.44 (d, J = 8.4 Hz, 2H), 6.90 (d, J = 7.8 Hz, 1H), 4.21 (s, 2H), 2.28 (s, 3H). ^{13}C NMR (150 MHz, MeOD- d_4) δ 162.7, 157.7,

148.7, 144.6, 144.0, 132.1, 131.9, 130.8, 130.5, 128.2, 128.0, 127.6, 126.3, 125.1, 117.2, 48.7, 17.6. IR (neat): ν 3442 (–OH), 3268 (–NH–), 1615 (–C=N–), 1591 (–N=N–), 1377 (–SO₂–). MS (m/z): calcd for C₂₁H₁₉F₃N₃O₃S⁺ [M + H]⁺, 450.11; found, 450.11. Purity >99%, t_R = 6.5 min. mp 181.8 °C.

(*E*)-4-((2-Amino-4-hydroxy-5-methylphenyl)diazenyl)-*N*-(4-(trifluoromethyl)benzyl)benzenesulfonamide (36). ¹H NMR (600 MHz, DMSO-*d*₆) δ 10.22 (s, 1H), 8.30 (t, J = 3.9 Hz, 1H), 7.90–7.80 (m, 4H), 7.64 (d, J = 8.4 Hz, 2H), 7.49 (d, J = 8.4 Hz, 2H), 7.41 (s, 1H), 7.19 (br s, 2H), 6.23 (s, 1H), 4.17 (d, J = 3.9 Hz, 2H), 2.02 (s, 3H). IR (neat): ν 3479 (–OH), 3233 (–NH–), 1631 (–C=N–), 1596 (–N=N–), 1389 (–SO₂–). MS (m/z): calcd for C₂₁H₂₀F₃N₄O₃S⁺ [M + H]⁺, 465.12; found, 465.12. Purity >99%, t_R = 6.3 min. mp 171.7 °C.

(*E*)-4-((4-Methoxy-3,5-dimethylphenyl)diazenyl)-*N*-(pyridin-2-yl)benzenesulfonamide (37). ¹H NMR (600 MHz, DMSO-*d*₆) δ 8.10–7.96 (m, 2H), 7.92–7.85 (m, 2H), 7.80–7.68 (m, 1H), 7.16–7.02 (m, 2H), 6.80–6.68 (m, 1H), 4.11 (s, 3H), 2.13 (s, 6H). MS (m/z): calcd for C₂₀H₂₁N₄O₃S⁺ [M + H]⁺, 397.13; found, 397.15. Yield: 3%, purity >99%, t_R = 6.2 min.

(*E*)-*N*-(2,6-Dimethyl-4-((4-(*N*-(pyridin-2-yl)sulfamoyl)phenyl)diazenyl)phenyl)acetamide (38). ¹H NMR (600 MHz, DMSO-*d*₆) δ 9.23 (s, 1H), 7.85–7.67 (m, 3H), 7.67–7.30 (m, 3H), 7.20–6.90 (m, 1H), 6.85–6.60 (m, 1H), 2.12 (s, 6H), 2.03 (s, 3H). MS (m/z): calcd for C₂₁H₂₂N₅O₃S⁺ [M + H]⁺, 446.14; found, 446.13. Yield: 5%, purity >99%, t_R = 5.0 min.

(*E*)-4-((4-Hydroxy-3-isopropylphenyl)diazenyl)-*N*-(pyridin-2-yl)benzenesulfonamide (39). ¹H NMR (600 MHz, DMSO-*d*₆) δ 10.46 (s, 1H), 8.08–7.99 (m, 3H), 7.91 (d, J = 7.8 Hz, 2H), 7.76 (m, 2H), 7.67 (d, J = 8.4 Hz, 2H), 7.22 (m, 1H), 6.98 (d, J = 8.4 Hz, 1H), 6.86 (m, 1H), 3.25 (m, 1H), 1.22 (d, J = 7.2 Hz, 6H). MS (m/z): calcd for C₂₀H₂₁N₄O₃S⁺ [M + H]⁺, 397.13; found, 397.13. Yield: 24%, purity >99%, t_R = 6.0 min.

(*E*)-4-((3-*tert*-Butyl-4-hydroxyphenyl)diazenyl)-*N*-(pyridin-2-yl)benzenesulfonamide (40). ¹H NMR (600 MHz, DMSO-*d*₆) δ 10.51 (s, 1H), 8.20–7.97 (m, 2H), 7.90 (d, J = 8.4 Hz, 2H), 7.84–7.65 (m, 4H), 7.40–7.10 (m, 1H), 6.98 (d, J = 8.4 Hz, 1H), 1.40 (s, 9H). MS (m/z): calcd for C₂₁H₂₃N₄O₃S⁺ [M + H]⁺, 411.15; found, 411.14. Yield: 20%, purity >99%, t_R = 6.2 min.

(*E*)-4-((4-Hydroxy-3,5-diisopropylphenyl)diazenyl)-*N*-(pyridin-2-yl)benzenesulfonamide (41). ¹H NMR (600 MHz, MeOD-*d*₄) δ 8.07 (d, J = 8.4 Hz, 2H), 8.01–7.96 (m, 1H), 7.93 (d, J = 8.4 Hz, 2H), 7.74 (t, J = 7.8 Hz, 2H), 7.70 (s, 2H), 7.30 (d, J = 8.4 Hz, 2H), 6.89 (t, J = 6.6 Hz, 1H), 3.45–3.60 (m, 2H), 1.28 (d, J = 7.2 Hz, 12H). MS (m/z): calcd for C₂₃H₂₇N₄O₃S⁺ [M + H]⁺, 439.18; found, 439.22. Yield: 16%, purity >99%, t_R = 6.3 min.

(*E*)-4-((3,5-di-*tert*-Butyl-4-hydroxyphenyl)diazenyl)-*N*-(pyridin-2-yl)benzenesulfonamide (42). ¹H NMR (600 MHz, MeOD-*d*₄) δ 8.01 (d, J = 6.6 Hz, 2H), 7.95 (d, J = 8.4 Hz, 1H), 7.73 (s, 2H), 7.57 (t, J = 7.2 Hz, 1H), 7.52 (d, J = 8.4 Hz, 2H), 7.29 (d, J = 9.0 Hz, 2H), 6.89 (t, J = 6.6 Hz, 1H), 1.37 (s, 9H), 1.31 (s, 9H). ¹³C NMR (150 MHz, MeOD-*d*₄) δ 156.6, 156.4, 153.6, 144.6, 144.5, 143.6, 136.6, 135.0, 131.3, 129.3, 126.8 (m), 125.9, 118.0, 117.5, 116.5, 37.1, 31.5, 31.3. MS (m/z): calcd for C₂₅H₃₁N₄O₃S⁺ [M + H]⁺, 467.21; found, 467.21. Yield: 2%, purity >99%, t_R = 6.8 min.

(*E*)-4-((4-Hydroxynaphthalen-1-yl)diazenyl)-*N*-(pyridin-2-yl)benzenesulfonamide (43). ¹H NMR (600 MHz, DMSO-*d*₆) δ 10.13 (s, 1H), 8.96–8.88 (m, 1H), 8.55–8.43 (m, 1H), 8.37–8.20 (m, 1H), 8.16–8.00 (m, 2H), 7.99–7.84 (m, 1H), 7.83–7.70 (m, 2H), 7.69–7.54 (m, 1H), 7.53–7.40 (m, 1H), 7.40–7.28 (m, 1H), 7.27–6.99 (m, 1H), 6.97–6.69 (m, 1H), 5.75 (s, 1H). MS (m/z): calcd for C₂₁H₁₇N₄O₃S⁺ [M + H]⁺, 405.10; found, 405.12. Yield: 67%, purity >99%, t_R = 5.0 min.

(*E*)-4-((4-Hydroxy-5,6,7,8-tetrahydronaphthalen-1-yl)diazenyl)-*N*-(pyridin-2-yl)benzenesulfonamide (44). ¹H NMR (600 MHz, MeOD-*d*₄) δ 8.04 (d, J = 8.6 Hz, 2H), 7.95 (d, J = 5.1 Hz, 1H), 7.87 (d, J = 8.5 Hz, 2H), 7.73 (td, J = 8.0, 1.9 Hz, 1H), 7.49 (d, J = 8.8 Hz, 1H), 7.28 (d, J = 8.8 Hz, 1H), 6.88 (t, J = 6.4 Hz, 1H), 6.65 (d, J = 8.8 Hz, 1H), 3.31–3.25 (m, 2H), 2.99 (s, 1H), 2.86 (s, 1H), 2.73–2.67 (m, 2H), 1.89–1.83 (m, 4H). HRMS (m/z): calcd for C₂₁H₂₁N₄O₃S⁺ [M + H]⁺, 409.133; found, 409.129. Purity >99%, t_R = 5.1 min.

(*E*)-4-((5-Hydroxy-1,2,3,4-tetrahydroquinolin-8-yl)diazenyl)-*N*-(pyridin-2-yl)benzenesulfonamide (45). ¹H NMR (600 MHz, DMSO-*d*₆) δ 8.03–7.95 (m, 1H), 7.87 (d, J = 8.5 Hz, 2H), 7.71 (td, J = 8.1, 1.9 Hz, 1H), 7.61 (d, J = 8.1 Hz, 2H), 7.15 (d, J = 7.9 Hz, 1H), 7.04 (d, J = 8.9 Hz, 1H), 6.86 (t, J = 6.4 Hz, 1H), 6.30 (d, J = 8.9 Hz, 1H), 3.32–3.24 (m, 2H), 3.16–3.14 (m, 2H), 1.76 (qt, J = 6.6 Hz, 2H). HRMS (m/z): calcd for C₂₀H₂₀N₅O₃S⁺ [M + H]⁺, 410.128; found, 410.126. Purity >96%, t_R = 4.7 min.

(*E*)-4-((7-Hydroxy-2,2-dimethyl-2,3-dihydrobenzofuran-4-yl)diazenyl)-*N*-(pyridin-2-yl)benzenesulfonamide (46). ¹H NMR (600 MHz, MeOD-*d*₄) δ 8.05 (d, J = 8.5 Hz, 2H), 7.95 (d, J = 4.8 Hz, 1H), 7.88 (d, J = 8.5 Hz, 2H), 7.74 (td, J = 8.1, 1.7 Hz, 1H), 7.37 (d, J = 8.6 Hz, 1H), 7.28 (d, J = 8.8 Hz, 1H), 6.89 (t, J = 6.4 Hz, 1H), 6.80 (d, J = 8.6 Hz, 1H), 3.42 (s, 2H), 1.52 (s, 6H). HRMS (m/z): calcd for C₂₁H₂₁N₄O₄S⁺ [M + H]⁺, 425.128; found, 425.124. Purity >99%, t_R = 4.8 min.

(*E*)-4-((5-Hydroxy-3-(hydroxymethyl)-4,6-dimethylpyridin-2-yl)diazenyl)-*N*-(pyridin-2-yl)benzenesulfonamide (47). ¹H NMR (600 MHz, MeOD-*d*₄) δ 8.10 (d, J = 8.5 Hz, 2H), 8.03 (d, J = 8.4 Hz, 2H), 7.95 (d, J = 5.1 Hz, 1H), 7.76 (ddd, J = 8.9, 7.2, 1.8 Hz, 1H), 7.31 (d, J = 8.9 Hz, 1H), 6.89 (t, J = 6.5 Hz, 1H), 5.18 (d, J = 0.8 Hz, 2H), 2.57 (s, 3H), 2.46 (s, 3H). HRMS (m/z): calcd for C₁₉H₂₀N₅O₄S⁺ [M + H]⁺, 414.123; found, 414.121. Purity >95%, t_R = 4.0 min.

(*E*)-4-((4-(Aminomethyl)-5-hydroxy-3-(hydroxymethyl)-6-methylpyridin-2-yl)diazenyl)-*N*-(pyridin-2-yl)benzenesulfonamide (48). ¹H NMR (600 MHz, MeOD-*d*₄) δ 8.04 (d, J = 7.1 Hz, 2H), 7.96 (d, J = 5.0 Hz, 1H), 7.92–7.79 (m, 2H), 7.74 (td, J = 8.0, 1.9 Hz, 1H), 7.28 (d, J = 8.7 Hz, 1H), 6.89 (t, J = 6.4 Hz, 1H), 5.17 (s, 2H), 4.28 (s, 2H), 2.51 (s, 3H). HRMS (m/z): calcd for C₁₉H₂₁N₆O₄S⁺ [M + H]⁺, 429.135; found, 429.136. Purity >95%, t_R = 2.2 min.

(*E*)-4-((4-Formyl-5-hydroxy-3-(hydroxymethyl)-6-methylpyridin-2-yl)diazenyl)-*N*-(pyridin-2-yl)benzenesulfonamide (49). ¹H NMR (600 MHz, DMSO-*d*₆) δ 7.99 (d, J = 4.4 Hz, 1H), 7.85 (d, J = 8.6 Hz, 2H), 7.64 (dd, J = 17.8, 8.0 Hz, 3H), 7.08 (d, J = 8.5 Hz, 1H), 6.79 (t, J = 5.8 Hz, 1H), 6.11 (s, 2H), 5.14 (d, J = 15.1 Hz, 1H), 4.95 (d, J = 15.2 Hz, 1H), 2.23 (s, 3H). HRMS (m/z): calcd for C₁₉H₁₈N₅O₅S⁺ [M + H]⁺, 428.103; found, 428.105. Purity >96%, t_R = 4.0 min.

(*E*)-4-((4-Hydroxy-3-methoxyphenyl)diazenyl)-*N*-(pyridin-2-yl)benzenesulfonamide (50). ¹H NMR (600 MHz, DMSO-*d*₆) δ 10.19 (s, 1H), 8.09–7.95 (m, 3H), 7.92 (d, J = 9.0 Hz, 2H), 7.77 (t, J = 6.0 Hz, 1H), 7.53 (d, J = 8.4 Hz, 1H), 7.46 (s, 1H), 7.24 (d, J = 9.0 Hz, 1H), 7.22 (m, 1H), 7.00 (d, J = 8.4 Hz, 1H), 6.87 (s, 1H), 3.83 (s, 3H). MS (m/z): calcd for C₁₈H₁₇N₄O₄S⁺ [M + H]⁺, 385.10; found, 385.05. Yield: 60%, purity >99%, t_R = 5.9 min.

(*E*)-3-((2-Amino-4-hydroxy-5-methylphenyl)diazenyl)-*N*-(pyridin-2-yl)benzenesulfonamide (51). ¹H NMR (600 MHz, DMSO-*d*₆) δ 8.15 (s, 1H), 8.04–7.92 (m, 2H), 7.76 (d, J = 7.8 Hz, 1H), 7.73 (t, J = 7.8 Hz, 1H), 7.59 (t, J = 7.8 Hz, 1H), 7.44 (s, 1H), 7.20 (d, J = 8.4 Hz, 1H), 6.84 (t, J = 6.0 Hz, 1H), 6.29 (s, 1H), 2.02 (s, 3H). ¹³C NMR (150 MHz, DMSO-*d*₆) δ 165.6, 156.6, 154.9, 149.9, 146.5, 144.2, 140.1, 133.8, 133.1, 131.1, 128.6, 127.8, 121.9, 119.9, 118.3, 117.5, 103.5, 18.5. MS (m/z): calcd for C₁₈H₁₈N₅O₃S⁺ [M + H]⁺, 384.11; found, 384.14. Yield: 86%, purity >99%, t_R = 4.7 min.

■ ASSOCIATED CONTENT

Supporting Information

Additional diazobenzene inhibitors and crystallography data and refinement statistics for BRD4–BrD1/MS436, BRD4–BrD1/MS435, and BRD4–BrD1/MS267. This material is available free of charge via the Internet at <http://pubs.acs.org>.

■ AUTHOR INFORMATION

Corresponding Author

*Phone: 212-659-8652; Fax: 212-849-2456; E-mail: ming-ming-zhou@mssm.edu.

Author Contributions

G.T.Z. and M.-M. Z. conceived and designed the experiments for this project. G.T.Z. and M.O. designed the synthetic

schemes, and G.T.Z performed the chemical synthesis. J.J. prepared the protein samples and carried out crystallization. A.N.P. solved the crystal structures. E.R., K.M., and L.Z. performed the biochemical binding study. T.S. and S.M. performed the cell biology study. G.T.Z. and M.-M.Z. wrote the manuscript.

Notes

The authors declare no competing financial interest.

ACKNOWLEDGMENTS

We acknowledge the use of the NMR facility at the New York Structural Biology Center and thank the staff at the X6A beamline of the National Synchrotron Light Sources at the Brookhaven National Laboratory for facilitating the X-ray data collection. This work was supported in part by research grants from the National Institutes of Health (to M.-M.Z.).

ABBREVIATIONS USED

Brd, bromodomain; NOS, nitric oxide synthase; iNOS, inducible nitric oxide synthase

REFERENCES

- (1) Kouzarides, T. Chromatin modifications and their function. *Cell* **2007**, *128*, 693–705.
- (2) Dhalluin, C.; Carlson, J. E.; Zeng, L.; He, C.; Aggarwal, A. K.; Zhou, M. M. Structure and ligand of a histone acetyltransferase bromodomain. *Nature* **1999**, *399*, 491–496.
- (3) Sanchez, R.; Zhou, M. M. The role of human bromodomains in chromatin biology and gene transcription. *Curr. Opin. Drug Discovery Dev.* **2009**, *12*, 659–665.
- (4) Filippakopoulos, P.; Picaud, S.; Mangos, M.; Keates, T.; Lambert, J. P.; Barsyte-Lovejoy, D.; Felletar, I.; Volkmer, R.; Muller, S.; Pawson, T.; Gingras, A. C.; Arrowsmith, C. H.; Knapp, S. Histone recognition and large-scale structural analysis of the human bromodomain family. *Cell* **2012**, *149*, 214–231.
- (5) Vidler, L. R.; Brown, N.; Knapp, S.; Hoelder, S. Druggability analysis and structural classification of bromodomain acetyl-lysine binding sites. *J. Med. Chem.* **2012**, *55*, 7346–7359.
- (6) Filippakopoulos, P.; Qi, J.; Picaud, S.; Shen, Y.; Smith, W. B.; Fedorov, O.; Morse, E. M.; Keates, T.; Hickman, T. T.; Felletar, I.; Philpott, M.; Munro, S.; McKeown, M. R.; Wang, Y. C.; Christie, A. L.; West, N.; Cameron, M. J.; Schwartz, B.; Heightman, T. D.; La Thangue, N.; French, C. A.; Wiest, O.; Kung, A. L.; Knapp, S.; Bradner, J. E. Selective inhibition of BET bromodomains. *Nature* **2010**, *468*, 1067–1073.
- (7) Nicodeme, E.; Jeffrey, K. L.; Schaefer, U.; Beinke, S.; Dewell, S.; Chung, C. W.; Chandwani, R.; Marazzi, I.; Wilson, P.; Coste, H.; White, J.; Kirilovsky, J.; Rice, C. M.; Lora, J. M.; Prinjha, R. K.; Lee, K.; Tarakhovskiy, A. Suppression of inflammation by a synthetic histone mimic. *Nature* **2010**, *468*, 1119–1123.
- (8) Zuber, J.; Shi, J. W.; Wang, E.; Rappaport, A. R.; Herrmann, H.; Sison, E. A.; Magoon, D.; Qi, J.; Blatt, K.; Wunderlich, M.; Taylor, M. J.; Johns, C.; Chicas, A.; Mulloy, J. C.; Kogan, S. C.; Brown, P.; Valent, P.; Bradner, J. E.; Lowe, S. W.; Vakoc, C. R. RNAi screen identifies Brd4 as a therapeutic target in acute myeloid leukaemia. *Nature* **2011**, *478*, 524–528.
- (9) Belkina, A. C.; Denis, G. V. BET domain co-regulators in obesity, inflammation and cancer. *Nat. Rev. Cancer* **2012**, *12*, 465–477.
- (10) Zhang, G.; Liu, R.; Zhong, Y.; Plotnikov, A. N.; Zhang, W.; Zeng, L.; Rusinova, E.; Gerona-Navarro, G.; Moshkina, N.; Joshua, J.; Chuang, P. Y.; Ohlmeyer, M.; He, J. C.; Zhou, M. M. Down-regulation of NF-kappaB transcriptional activity in HIV-associated kidney disease by BRD4 inhibition. *J. Biol. Chem.* **2012**, *287*, 28840–28851.
- (11) Tang, X.; Peng, R.; Phillips, J. E.; Deguzman, J.; Ren, Y.; Apparsundaram, S.; Luo, Q.; Bauer, C. M.; Fuentes, M. E.; Demartino, J. A.; Tyagi, G.; Garrido, R.; Hogaboam, C. M.; Denton, C. P.;

Holmes, A. M.; Kitson, C.; Stevenson, C. S.; Budd, D. C. Assessment of Brd4 inhibition in idiopathic pulmonary fibrosis lung fibroblasts and in vivo models of lung fibrosis. *Am. J. Pathol.* **2013**, *183*, 470–479.

(12) Huang, B.; Yang, X. D.; Zhou, M. M.; Ozato, K.; Chen, L. F. Brd4 coactivates transcriptional activation of NF-kappaB via specific binding to acetylated RelA. *Mol. Cell. Biol.* **2009**, *29*, 1375–1387.

(13) Schroder, S.; Cho, S.; Zeng, L.; Zhang, Q.; Kaelcke, K.; Mak, L.; Lau, J.; Bisgrove, D.; Schnolzer, M.; Verdin, E.; Zhou, M. M.; Ott, M. Two-pronged binding with bromodomain-containing protein 4 liberates positive transcription elongation factor b from inactive ribonucleoprotein complexes. *J. Biol. Chem.* **2012**, *287*, 1090–1099.

(14) Hewings, D. S.; Fedorov, O.; Filippakopoulos, P.; Martin, S.; Picaud, S.; Tumber, A.; Wells, C.; Olcina, M. M.; Freeman, K.; Gill, A.; Ritchie, A. J.; Sheppard, D. W.; Russell, A. J.; Hammond, E. M.; Knapp, S.; Brennan, P. E.; Conway, S. J. Optimization of 3,5-dimethylisoxazole derivatives as potent bromodomain ligands. *J. Med. Chem.* **2013**, *56*, 3217–3227.

(15) Seal, J.; Lamotte, Y.; Donche, F.; Bouillot, A.; Mirguet, O.; Gellibert, F.; Nicodeme, E.; Krysa, G.; Kirilovsky, J.; Beinke, S.; McCleary, S.; Rioja, I.; Bamborough, P.; Chung, C. W.; Gordon, L.; Lewis, T.; Walker, A. L.; Cutler, L.; Lugo, D.; Wilson, D. M.; Witherington, J.; Lee, K.; Prinjha, R. K. Identification of a novel series of BET family bromodomain inhibitors: Binding mode and profile of I-BET151 (GSK1210151A). *Bioorg. Med. Chem. Lett.* **2012**, *22*, 2968–2972.

(16) Dawson, M. A.; Prinjha, R. K.; Dittmann, A.; Giotopoulos, G.; Bantscheff, M.; Chan, W. I.; Robson, S. C.; Chung, C. W.; Hopf, C.; Savitski, M. M.; Huthmacher, C.; Gudgin, E.; Lugo, D.; Beinke, S.; Chapman, T. D.; Roberts, E. J.; Soden, P. E.; Auger, K. R.; Mirguet, O.; Doehner, K.; Delwel, R.; Burnett, A. K.; Jeffrey, P.; Drewes, G.; Lee, K.; Huntly, B. J. P.; Kouzarides, T. Inhibition of BET recruitment to chromatin as an effective treatment for MLL-fusion leukaemia. *Nature* **2011**, *478*, 529–533.

(17) Bamborough, P.; Diallo, H.; Goodacre, J. D.; Gordon, L.; Lewis, A.; Seal, J. T.; Wilson, D. M.; Woodrow, M. D.; Chung, C. W. Fragment-based discovery of bromodomain inhibitors part 2: Optimization of phenylisoxazole sulfonamides. *J. Med. Chem.* **2012**, *55*, 587–596.

(18) Borah, J. C.; Mujtaba, S.; Karakikes, I.; Zeng, L.; Muller, M.; Patel, J.; Moshkina, N.; Morohashi, K.; Zhang, W. J.; Gerona-Navarro, G.; Hajjar, R. J.; Zhou, M. M. A small molecule binding to the coactivator CREB-binding protein blocks apoptosis in cardiomyocytes. *Chem. Biol.* **2011**, *18*, 531–541.

(19) Perola, E. An analysis of the binding efficiencies of drugs and their leads in successful drug discovery programs. *J. Med. Chem.* **2010**, *53*, 2986–2997.

(20) Tarcsay, A.; Keseru, G. M. Contributions of molecular properties to drug promiscuity miniperspective. *J. Med. Chem.* **2013**, *56*, 1789–1795.

(21) Hughes, J. D.; Blagg, J.; Price, D. A.; Bailey, S.; DeCrescenzo, G. A.; Devraj, R. V.; Ellsworth, E.; Fobian, Y. M.; Gibbs, M. E.; Gilles, R. W.; Greene, N.; Huang, E.; Krieger-Burke, T.; Loesel, J.; Wager, T.; Whiteley, L.; Zhang, Y. Physicochemical drug properties associated with in vivo toxicological outcomes. *Bioorg. Med. Chem. Lett.* **2008**, *18*, 4872–4875.

(22) Lee, K. H.; Kim, D. G.; Shin, N. Y.; Song, W. K.; Kwon, H.; Chung, C. H.; Kang, M. S. NF-kappa B-dependent expression of nitric oxide synthase is required for membrane fusion of chick embryonic myoblasts. *Biochem. J.* **1997**, *324*, 237–242.

(23) Belkina, A. C.; Nikolajczyk, B. S.; Denis, G. V. BET protein function is required for inflammation: Brd2 genetic disruption and BET inhibitor JQ1 impair mouse macrophage inflammatory responses. *J. Immunol.* **2013**, *190*, 3670–3678.

(24) Fish, P. V.; Filippakopoulos, P.; Bish, G.; Brennan, P. E.; Bunnage, M. E.; Cook, A. S.; Federov, O.; Gerstenberger, B. S.; Jones, H.; Knapp, S.; Marsden, B.; Nocka, K.; Owen, D. R.; Philpott, M.; Picaud, S.; Primiano, M. J.; Ralph, M. J.; Sciammetta, N.; Trzupke, J. D. Identification of a chemical probe for bromo and extra C-terminal

bromodomain inhibition through optimization of a fragment-derived hit. *J. Med. Chem.* **2012**, *55*, 9831–9837.

(25) Nikolovska-Coleska, Z.; Wang, R.; Fang, X.; Pan, H.; Tomita, Y.; Li, P.; Roller, P. P.; Krajewski, K.; Saito, N. G.; Stuckey, J. A.; Wang, S. Development and optimization of a binding assay for the XIAP BIR3 domain using fluorescence polarization. *Anal. Biochem.* **2004**, *332*, 261–273.

(26) Otwinowski, Z.; Minor, W. Processing of X-ray diffraction data collected in oscillation mode. In *Methods in Enzymology*; Carter, C. W., Jr., Ed.; Academic Press: San Diego, CA, 1997; Vol. 276, pp 307–326.

(27) Vagin, A.; Teplyakov, A. . MOLREP: An automated program for molecular replacement. *J. Appl. Crystallogr.* **1997**, *30*, 1022–1025.

(28) Murshudov, G. N.; Vagin, A. A.; Dodson, E. J. Refinement of macromolecular structures by the maximum-likelihood method. *Acta Crystallogr., Sect. D* **1997**, *53*, 240–255.

(29) Emsley, P.; Cowtan, K. Coot: Model-building tools for molecular graphics. *Acta Crystallogr., Sect. D* **2004**, *60*, 2126–2132.

(30) Hunger, K.; Mischke, P.; Rieper, W. Azo dyes. In *Ullmann's Encyclopedia of Industrial Chemistry*; Wiley-VCH: Weinheim, Germany, 2000.

(31) Zhou, M. M.; Ohlmeyer, M.; Mujtaba, S.; Plotnikov, A.; Kastrinsky, D.; Zhang, G.; Borah, J. Inhibitors of bromodomains as modulators of gene expression. Patent WO2012116170, 2012.

(32) Wallace, A.; Laskowski, R.; Thornton, J. LIGPLOT: A program to generate schematic diagrams of protein-ligand interactions. *Protein Eng.* **1995**, *8*, 127–134.